Renewable and Sustainable Energy Reviews 217 (2025) 115716

Contents lists available at ScienceDirect

Renewable and Sustainable Energy Reviews

journal homepage: www.elsevier.com/locate/rser

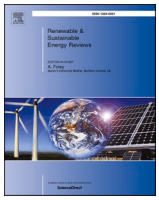

Development of an analytical model of automobile energy consumption during use-phase for parametrized life cycle assessment

Gabriel Magnaval *, Anne-Marie Boulay

CIRAIG, Department of Chemical Engineering, Polytechnique Montreal, 2500, Chem. De Polytechnique, Montreal, Canada

ARTICLE INFO

Keywords:
Life cycle assessment
Automobile energy consumption
Parametrization
Lightweighting

ABSTRACT

Models for automobile energy consumption calculations often lack adaptability, granularity, and consistency, limiting the transparency, reproducibility, and representativeness of automobile processes in Life Cycle Assessment (LCA). Although developing parametrized models appears to be promising, their application to automobile energy consumption is constrained by the complexity of powertrain modeling and the integration of driving conditions. This work presents a model for gasoline and electric vehicles based on parametrized equations, describing physical drivers of energy demand while uncoupling the role of contributors, including the vehicle body, powertrain, path, and driver. An innovative method for parametrizing driving conditions is introduced, eliminating reliance on traditional driving cycles. Complemented by pre-set configurations to enhance usability, the computational tool *PETRAUL* built on this framework enables practitioners to perform precise and representative energy consumption calculations for vehicles. This study further demonstrates the tool's utility for both foreground and background LCA processes. This includes scenario analyses emphasizing the necessity of multi-solution strategies, a comparison with *ecoinvent and Carculator* highlighting improved granularity, and an LCA case study on lightweighting, illustrating enhanced representativeness for assessments across diverse technological and regional conditions. This streamlined LCA of a polycarbonate glazing highlights the potential burden shifting from the vehicle use phase to the manufacturing of lightweight materials, notably when coupled with electrification. Ultimately, PETRAUL provides a robust foundation for advancing LCA practices by enhancing adaptability and transparency in parametrized modeling, while illustrating the need for both technological and sobriety measures to reduce environmental impacts of the automobile industry.

1. Introduction

The vehicle industry stands as a significant anthropogenic source of pollution. Road transportation accounted for approximately 10 % of global CO2 emissions in 2019 [1]. Acknowledging the magnitude of this environmental challenge, the industry has made efforts to implement innovative technologies and sustainable practices [2]. Improvements aimed at mitigating emissions can reduce impacts at different stages of the life cycle of a vehicle. Assessing the environmental impacts of these changes is crucial to support the industry's efforts and to inform stakeholders of the most promising strategies for reducing emissions. Life Cycle Assessment (LCA) is a relevant tool to quantify impacts along the life cycle of automobiles. Existing LCAs of automobiles prove that energy transformation and consumption for the use phase have a major contribution to impacts, especially for Internal Combustion Engine Vehicles (ICEV) [3–7]. Therefore, manufacturers, public authorities, and consumers should get involved to explore and develop potential solutions for reducing the energy consumption of vehicles through technological innovations, policy regulations, and consumer behavior changes [8–10]. Building LCA on accurate and consistent energy consumption evaluation models is crucial to precisely evaluate and adequately compare these solutions.

ecoinvent is a reference Life Cycle Inventory (LCI) database that combines data on more than 20,000 processes [11]. It contains a category of processes representative of automobile transport. These processes are built according to two distinct models in the latest version 3 of *ecoinvent*: one for ICEV [3] and one for Battery Electric Vehicles (BEV) [6]. The representativity (technological, temporal, and geographical) and the consistency of energy consumption calculation for these methods can be questioned. For ICEV, practitioners can select among three types of ICEV (gasoline vehicles (GV), diesel vehicles (DV), natural gas vehicles (NGV)), three sizes of car bodies (small, medium, large), and three levels of emissions (EURO3, EURO4, EURO5), while only one

* Corresponding author.
E-mail address: gabriel.magnaval@polymtl.ca (G. Magnaval).

https://doi.org/10.1016/j.rser.2025.115716
Received 15 February 2025; Received in revised form 3 April 2025; Accepted 5 April 2025
Available online 19 April 2025

List of abbreviations

BEV	Battery Electric Vehicle
DV	Diesel Vehicle
EEA	European Environmental Agency
EPA	United States Environmental Protection Agency
FRV	Fuel Reduction Value
FTP75	Federal Test Procedure 75 (EPA)
GV	Gasoline Vehicle
HEV	Hybrid Electric Vehicle
HWFET	EPA Highway Fuel Economy Test
ICEV	Internal Combustion Engine Vehicle
JC08	Japan Cycle 08
LCA	Life-Cycle Assessment
LCI	Life-Cycle Inventory
MIEC	Mass Influence on Energy Consumption
MIF	Mass Induced Fuel
NEDC	New European Driving Cycle
PIEC	Parameter Influence on Energy Consumption
SC03	Supplementary Cycle 03 (EPA)
US06	United States Cycle 06 (EPA)
WLTP	Worldwide harmonized Light vehicles Test Procedure

scenario is available for BEV. This is insufficient to represent today's market diversity. The models are outdated – they date to 2016 – and do not allow for an accurate representation of production specificities or driving behavior disparities across regions. Regarding consistency, the modeling of ICEV and BEV is partially based on different assumptions (driving cycles, passenger weight), limiting the meaningfulness of comparisons.

A lack of adaptability of the models may explain these limits. The adaptability of an inventory refers to its ability to respond flexibly to evolving requirements, contexts, and user needs [12]. Adaptability allows for speeding up data collection, both for primary and secondary data [7]. However, LCA practices tend to favor the production of static LCIs as "snapshots", where flow interactions are implicit, complexifying updates within the models [13,14]. *ecoinvent* typically relies on the commercial driving simulation software TREMOVE [15] to estimate automobile energy consumption. However, since the software is not linked to the ecoinvent inventory, any adjustment requires recalculations within the software. This makes it more difficult for database managers to update the model and for practitioners to adapt the aggregated process to their product systems.

The development of parametrized frameworks has yielded promising results for improving the adaptability and transparency of LCA datasets [16,17]. An LCA parametrization approach consists of structuring a product's Life Cycle Inventory with relevant parameters that can be easily adjusted depending on the context [18]. Parametrization of LCIs has been applied in different fields [18–24], notably in the automotive industry [7,25,26]. An important question when parametrizing LCI is to determine the level of detail of the datasets [27,28]. Higher details mean capturing the underlying complexity of a system at a finer scale, by increasing the resolution or the granularity of the data collection. Detailing an LCI reduces the uncertainty of the impact results but is time-consuming [29]. The balance between preciseness and efficiency depends on the scope of a study [30,31]. For example, comparing two automobile pieces requires a more granulated model than studying an automobile fleet. So far, the modeling of the automobile energy consumption in the parametrized LCA models lacks precision and granularity for refined assessments. Models aggregate and thus mask influences of individual aspects, such as engine components or automobile design, as well as the interactions between the car and the driving conditions (path characteristics, driver behavior, etc.). Consequently, these parametrized models cannot be used to assess the sustainability of key industrial questions at a finer scale, like components lightweighting, engine downsizing, or eco-driving. Developing a parametrized and granular model, in which the LCI dataset's level of detail can be adapted to the practitioner's needs – as shown in other fields [30,32] – would increase the consistency of automotive LCAs.

This paper aims to build an adaptable and consistent method to estimate the energy consumption of automobiles based on a parametrized approach. To reach it, we propose.

1. To review the methods that have been developed in impact assessment to calculate the energy consumption of the automobile, to clearly identify the research gaps that limit the parametrization of this process, and to assess the potential benefits of such a parametrized approach for the field.
2. To develop an original parametrized method for energy consumption that bridges the research gaps identified in the review.
3. To validate the model and to generate pre-set configurations based on existing empirical measurements.
4. To create a tool for automobile energy consumption calculation designed for LCA practitioners and illustrate its use on a set of exemplary applications.

2. Existing models for energy consumption calculation and limitations

A comparative study of fourteen specific models [25,33–45] developed to estimate car energy consumption has been conducted. Six methods focus solely on ICEV [33,37,38,41,43,44], while eight others also adapted and applied their model to BEV [39,40,42,45–48] with one covering 9 types of engines, including Hybrid Engine Vehicles (HEV) [25]. The models are generally divided into three phases: i-external force analysis, ii-powertrain losses analysis, and iii-integration of dynamic parameters.

2.1. External forces

Four main external forces are described in the models: rolling friction, aerodynamic drag, automobile inertia, and wheel inertia. The road slope is also regularly mentioned but neglected during the integration phase [25,33,41,44]. Authors use widely accepted parametrized equations to describe external forces. Other forces, like wind force, and road curvature, are sometimes mentioned but never calculated.

2.2. Powertrain losses

The powertrain comprises an engine, a drivetrain (which includes a transmission and a driveline), and energy storage for BEV/HEV. The notion of efficiency, defined as the ratio between output power and input power of a system, is commonly used to describe powertrain components. Each element of the powertrain is defined by its own efficiency. Regenerative braking, which corresponds to kinetic energy recovery during braking, can also be characterized by an efficiency value. Efficiencies are dynamic variables that evolve over time based on driving conditions such as speed, load, and acceleration patterns. A distinction between four types of efficiency has been found in the studies. The *indicated efficiency* aggregates all thermodynamic and combustion losses; the *operating efficiency* computes the friction losses that depend on the operating point (torque and engine speed); the *differential efficiency* computes all losses that are invariant to the operating point; and the *total efficiency* computes the overall efficiency by multiplying differential and operating efficiencies [33,37,38,48].

Accurately estimating efficiencies is challenging as it requires accounting for the driving conditions. A first option is to calculate an average value for indicated [34,44], differential [37], or total efficiency [25,38,43] from literature sources. Averaging efficiency simplifies

calculations and enhances usability, making it ideal for low-resolution analyses. However, it hides the influence of operating conditions and technological variations, making it inappropriate for context-specific assessment.

A second option is to perform a graphical representation of efficiency with empirical efficiency maps [35,36,39,42,45]. Efficiency maps are embedded in simulation tools to obtain the real-time total efficiency of the powertrain. Efficiency maps increase the study's representativeness as they are based on empirical datasets. Yet, they do not make explicit causal links between the parameters and require the use of software or algorithms to integrate the measurements. Such software reduces both the transparency - by acting like black boxes - and the adaptability of the studies, as observed with the software TREMOVE.

Currently, averaging and graphical options are largely favored for engine modeling, but both methods are limited by their lack of adaptability and transparency. These limitations are made worse by inconsistent notation and terminology describing these efficiencies. It leads to inconsistencies and misunderstandings in powertrain modeling. The choice to use indicated efficiency, total efficiency, or other is often insufficiently justified. The disagreement between Kim et al. and Rohde-Brandenburger & Koffler on the influence of mass on operating efficiency demonstrates the need to better characterize the dependencies in efficiency calculation [49,50].

To address these limitations, a third option would be to adopt a parametrized approach. For internal combustion engines, parametrized equations have been developed to describe some of the losses, including thermodynamic losses [33,38], mechanical frictions using the Willans line approximation [33,34,37,51–53], and power demand of accessories and auxiliaries [25,42]. However, other losses - such as pumping and insulation - have not been parametrized in the literature, which means a fully parameterized method for these engines is not yet feasible. Additionally, for components like electric engines, drivetrains, and batteries, none of the methods reviewed proposes parametrized approaches. Overall, further development or completion of parametrized powertrain models is necessary to provide practitioners with a viable alternative to averaging and simulation methods.

2.3. Integration of dynamic parameters

Mathematically, the dynamic parameters should be integrated to calculate energy consumption from power demand. This includes the vehicle's speed and acceleration, the engine's rotation speed and torque, as well as environmental characteristics such as road slope and wind speed. These dynamic parameters depend on the driving conditions. This step is often referred to as the *simulation* in the literature, as a real-time calculation of energy consumption is performed with dynamic parameters simulated using driving cycles. A driving cycle is a standardized sequence that represents the typical speed of a vehicle in a driving scenario. Several cycles have been created worldwide to reflect characteristics specific to different regions. Currently, the WLTP, the EPA-FTP75, and the JC08 are the reference cycles, respectively, in Europe, North America, and Japan [54,55]. The use of driving cycles in energy models has certain limits. They are non-parametrized scenarios, which reduces the adaptability of the models. Furthermore, their representativity for real-world driving conditions is questionable as driving cycles underestimate energy consumption and other emissions like NOx [56,57]. They do not include driver behavior or traffic, nor environmental factors such as wind or slope [54,58], which leads to practitioners neglecting these external forces. The relative error in energy consumption between driving cycles and real-driving conditions is assessed to be between 13 and 76 % [59,60]. The scandal surrounding the Dieselgate emissions cheating software has also raised concerns about the integrity of vehicle emissions tests [61]. To overcome these limitations, VECTO model [39] proposed building path profiles based on empirical measurements which uncouple the "path target speed profile" from the driver behavior. However, these scenarios are not parametrized and cannot be generalized. Sciarretta et al. [45] developed parametrized paths for an optimization method. Yet, the model is highly detailed and requires a software for real-time quantification and calculation of dozens of dynamic parameters to finally obtain the energy consumption. This parametrization is not efficient enough for LCI development. Consequently, an innovative method should be developed to parametrize the integration of dynamic parameters.

2.4. Research gaps and contribution of this paper

The modeling of powertrain losses and the integration of driving conditions were identified by the literature review as the two main research gaps that limit the parametrization of automobile energy consumption.

While previous methods modeled powertrain losses with graphical efficiency maps or with average efficiency values, this work aims to develop a finer parametrized approach for powertrain losses, which would enable (1) to build a consistent and adaptable methodology for both ICEV and BEV; (2) to standardize the definition and the expression of efficiencies by identifying the powertrain losses that are proportional to the power supplied by the powertrain from other losses. It would propose a solution to the disagreement between Rohde-Brandenburger et al. [49] and Kim et al. [50] on the influence of mass on efficiency.

Driving conditions are mainly modeled by the controversial driving cycles in the literature. Rather than relying on simulation, this work aims to develop a novel approach, referred to as *parametrized integration of driving conditions*, to obtain a parametrized equation for integrating dynamic parameters. This approach would make it possible to (1) integrate certain hitherto neglected forces, typically road slope and wind effects; (2) uncouple the role of the driver and the role of the driving environment; and (3) produce customized driving scenarios, for example, to represent mountainous terrain, an aggressive driving style, or prospective driving scenarios.

Consequently, this paper presents a fully parametrized model, which required formulating the powertrain operation into equations—a complex task due to limited literature, non-linear behaviors, and intricate internal dynamics. It also involved overcoming the widespread reliance on standard driving cycles by developing a new set of useable equations to represent driving conditions, despite the scarcity of existing data and prior work on this topic. These innovative approaches coupled with existing equations for external forces result in an analytical expression of automotive energy consumption. These equations uncouple the automotive body, the powertrain elements, the path characteristics, and the driver behavior, making it possible to independently model each of these contributors. Additional contributions complement this parametrized model. In this paper, the model is compared with empirical datasets to validate the equations and assess the uncertainty of the results. Pre-set configurations are generated to improve the granularity and the usability of the model. The resulting equations and pre-set configurations are implemented in an online tool to reinforce the usability of the model. The tool is tested on exemplary case studies to illustrate its benefits and applicability to environmental assessment.

3. Methodology

This section describes the novel approach developed to assess the energy consumption of automobiles. The scope of the paper is limited to GV and BEV, but the methodology can be adapted to other powertrains (e.g., HEV, DV). The methodology is divided into three parts, plus the literature review as a preliminary step (objective 1, in green), as illustrated in Figure 1. Each part addresses one objective presented in the introduction.

The first part (in red, objective 2) consists of developing a parametrized model of energy consumption calculation for automobiles by describing the physical drivers (e.g., aerodynamic losses or engine losses) related to energy consumption using physics-based equations.

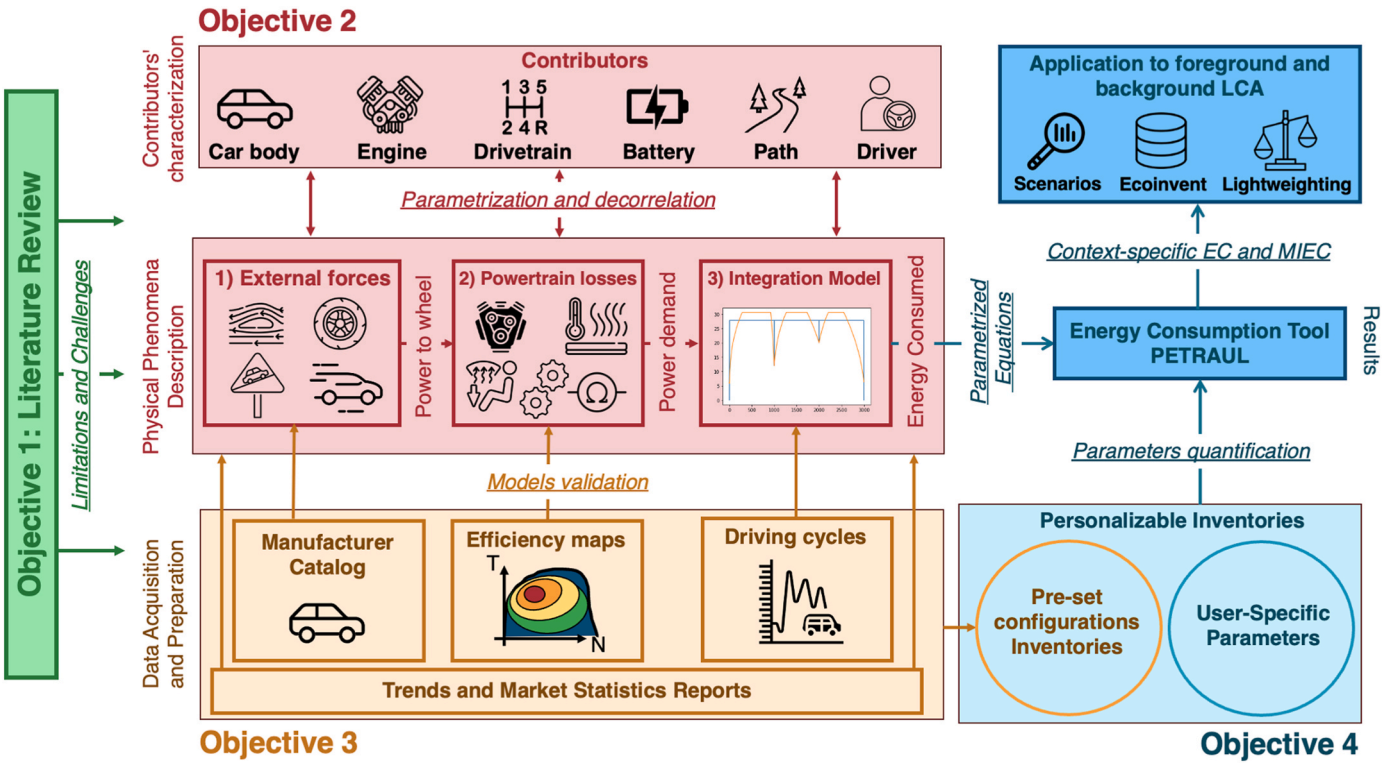

Figure 1. Graphical representation of the methodology. The literature review is performed to identify the limitations and challenges of existing models (objective 1, in green). The energy consumption of automobiles is modeled by parametrizing the process using physics-based equations (objective 2, in red). These parameters represent various contributors to energy consumption. The model is validated using empirical data from manufacturers and literature, which also provide pre-set configurations for each contributor (objective 3, in yellow). The equations are compiled into a tool that calculates energy consumption (EC) and Mass Influence on Energy Consumption (MIEC), allowing parameters to be quantified through either pre-set configurations or practitioner-specific inputs (objective 4, in blue). (For interpretation of the references to color in this figure legend, the reader is referred to the Web version of this article.)

Relevant parameters are introduced to characterize the contributors, meaning the most relevant determinants (e.g., the car, the powertrain, the driver, or the path characteristics) involved in the driving [36,42]. The second part (in orange, objective 3) consists of collecting and preparing data from the literature, manufacturers, and agencies involved in vehicle testing to validate the model. Moreover, pre-set configurations that describe reference categories of contributors were developed based on the data acquired. The third part (in blue, objective 4) consists of implementing equations in a user-friendly tool, called *PETRAUL*, that enables the computing of automobile energy consumption. LCA practitioners have the choice of using pre-set parameters developed in the second methodological part or their own specific parameters. Examples illustrate the use of *PETRAUL* for foreground and background LCA using scenario analyses and an application for lightweighting. They highlight the benefits of this paper's approach versus *ecoinvent* modeling and inform consumers and decision-makers on the most efficient energy-reduction approaches for automobiles. The following sections detail the three methodological steps of the paper.

3.1. Parametrized model for energy consumption

As observed in existing models, the mathematical description of the process relies on two steps: (1) the power required to overcome external forces and the powertrain losses from energy conversion (tank-to-wheels) are expressed and summed to determine the car's power demand as a function of time; (2) this power demand is integrated over time to calculate the energy consumed; and (3) the influence of a given parameter on the energy consumption can be derived from the used equations by calculating the Parameter Influence on Energy Consumption (PIEC). The following sections present the equations and assumptions used, as well as the key contributors influencing energy consumption. These contributors are categorized as technological (car body, engine, drivetrain, and storage for BEV) and dynamic (driver behavior and path characteristics).

3.1.1. Power demand modeling

In this first step, physical drivers of power demand are expressed using analytical equations selected from existing models and specialized literature, based on the following criteria.

- Each equation must be validated by at least two sources to ensure consistency and reliability.
- Granularity must be ensured by using raw parameters that uncouple individual contributors, avoiding hidden dependencies and accurately reflecting specific contributions. Some simplifications are allowed to maintain usability.
- Process-based equations are prioritized over empirical ones to better understand parameter relationships and enhance result transparency and interpretability.

Furthermore, in this model, powertrain losses are not uniformly represented as efficiency. While being a common practice in the automotive industry, representing losses as efficiency assumes that all powertrain losses are proportional to power consumption, coupling engine-characteristic parameters with engine dynamics. Instead, this paper uses the term *loss* to capture the fact that some powertrain losses are independent of power demand and must be treated as separate contributions to automobile consumption. The term *efficiency* is limited to *differential efficiency*, which describes losses proportional to power demand, as defined by Rohde-Brandenburger et al. [49,53].

Based on these criteria, a comprehensive set of equations has been developed to model power demand. The following paragraphs

summarize the main losses considered and the sources used to parametrize their influence. Detailed explanations and equations can be found in **Supplementary Information SI-1**.

(A) External forces include rolling friction, aerodynamic drag, automobile inertia, wheel inertia, and road slope using widely accepted expressions. Wind force is also added based on specific studies [42,62,63].
(B) Gasoline engine losses include thermodynamic, friction, thermal, injection, and pumping losses, as described by Ross (1997) [33], with refinements from specialized papers [64–68]. A cold-start energy loss is also added [69].
(C) Electric engine losses include copper loss, core loss, converter losses, and mechanical losses, with expressions derived from empirical experiments conducted by Mahmoudi et al. (2015) [70] and Roshandel et al. (2021) [71].
(D) Drivetrain losses include driveline losses [72] and transmission losses, namely friction losses [73] and synchronization losses [73, 74].
(E) Storage losses, specific to BEV, include charging losses due to AC to DC conversion [75–77] and discharging losses caused by internal battery resistance [77–79].
(F) Regenerative braking losses, specific to BEV, include mechanical braking used at high deceleration rates for security reasons [80, 81].
(G) Accessory demand includes electrical power for the engine, heating in cold weather, and air-conditioning in warm weather as proposed by Sacchi et al. [25].

3.1.2. *Integration of power demand*

Obtaining energy consumption from power demand equations requires an integration of the equations' dynamic parameters of power equations. This section introduces an innovative *parametrized integration* method. In this method, dynamic variables are expressed as functions of the distance traveled. Inspired by the VECTO model [39], the method distinguishes between *target functions*, determined solely by the path, and *real functions*, which incorporate driver behavior. The road is divided into segments with constant driving conditions to facilitate the definition of parameters characterizing these sections. Each section is characterized by a set distance d_{sect}. To model the impact of the driver, road sections are decomposed into three phases: acceleration, cruising, and braking. Parameters are introduced to characterize the driver aggressiveness during these three phases.

The method is presented in two steps. First, the models, the assumptions (A1 to A7), and the parameters introduced to develop the

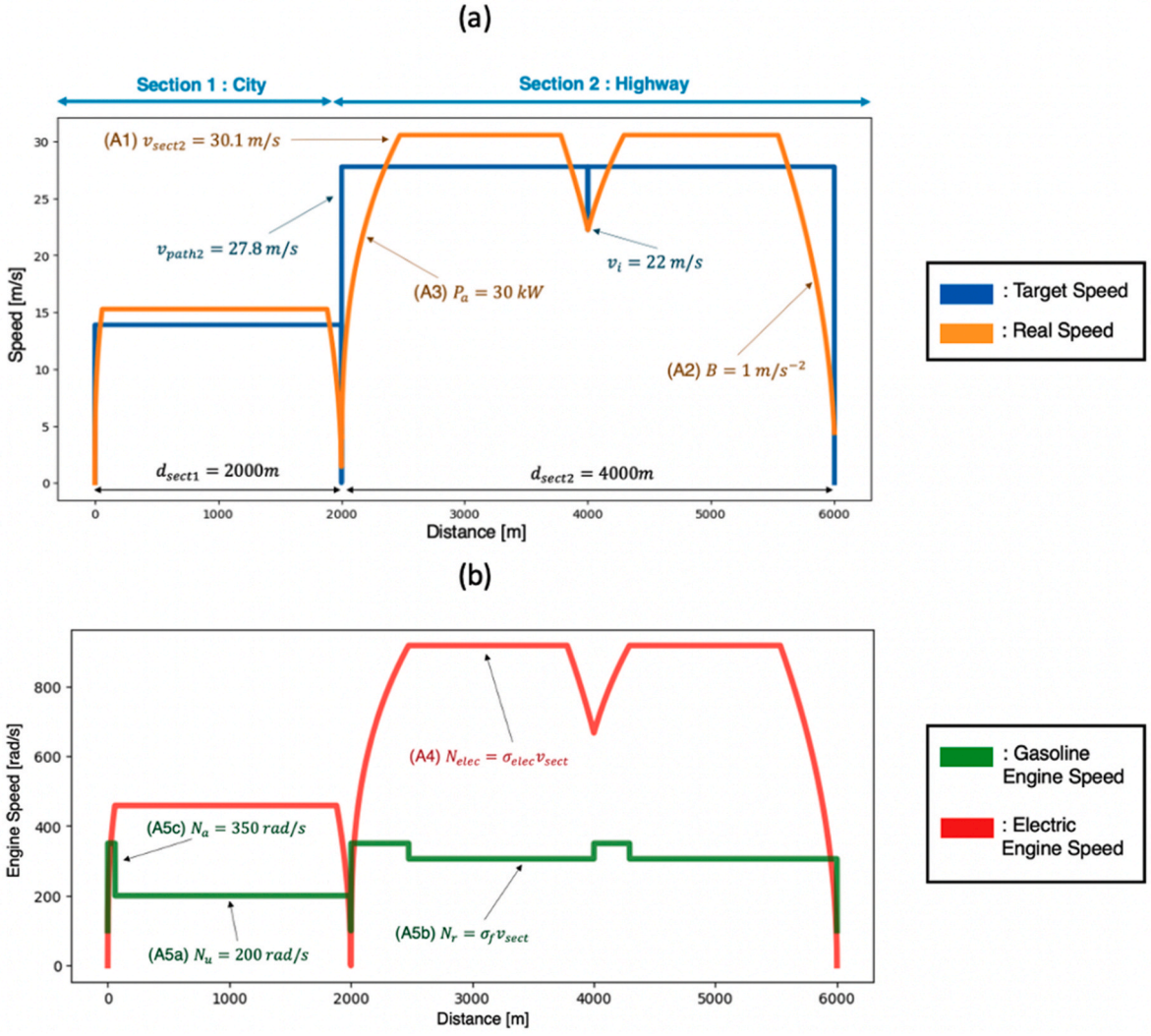

Figure 2. Graphical Representation of the Integration Method for a theoretical travel of 6 km with 2 km of urban travel and 4 km of highway travel. a) represents the target speed (in blue) and the real speed (in orange) functions, and b) represents the real engine speed functions for ICEV and BEV. (For interpretation of the references to color in this figure legend, the reader is referred to the Web version of this article.)

target and *real functions* of the dynamic variables are presented. Second, the method to calculate the integrals of the dynamic parameters from these functions is developed.

1 Assumptions and parameters introduced

Some assumptions and parameters introduced are represented in Figure 2, which depicts an illustrative journey consisting of 2 km of urban travel and 4 km of highway travel.

First, for the *target speed*, a constant target cruise speed v_{path} is defined for each segment, which can be interpreted as the speed limit of the road. Specific incidents causing punctual speed reductions v_i are also introduced. Acceleration and braking are neglected at that stage. This structure results in a rectangular function for the *target speed* (see the blue curve in Figure 2a). To convert the *target speed* into *real speed*, the driver behavior during cruise, braking, and acceleration is modeled through three assumptions A1-A3:

(A1) *Cruise*: A constant cruise speed of the vehicle is assumed, neglecting minor speed fluctuations. These fluctuations are disregarded as they correspond to the natural deceleration of the vehicle due to friction and do not significantly affect inertia computation. The *real* cruise speed (v_{sect}) is defined in Equation (1) with the ratio μ_v characterizing the driver's compliance with speed regulations (v_{path}).

$$v_{sect} = \mu_v . v_{path} \quad \text{(Equation 1)}$$

(A2) *Braking*: It is assumed that the driver steadily slows the vehicle using constant brake pressure. This results in a uniform deceleration, denoted as B, which is a driver-specific parameter reflecting their braking aggressiveness.

(A3) *Acceleration*: A continuous increase in speed is modeled by assuming constant power applied to the vehicle. This power, denoted as P_a, is defined in Equation (2) where P_e is the maximum power available from the engine and μ_a represents the driver's utilization rate of this power, reflecting aggressiveness during acceleration phases. The impact of the driver on the real speed functions is represented in Figure (2a) (orange curve).

$$P_a = \mu_a P_e \quad \text{(Equation 2)}$$

Second, the engine speed (N) which corresponds to the angular speed of the engine's rotational motion, is expressed in the literature using Equation (3) as a function of the drive ratio ($\sigma_t(t)$) and the vehicle speed (v) [36]. This drive ratio is determined by the gearbox ratio (trans_f), the engaged gear ratio ($\text{trans}_g(t)$) and the radius of the wheel (r_w). To simplify the complexity of gear shifting, which is influenced by the engine, transmission, and driver behavior, assumptions A4 and A5 are introduced.

$$N = \frac{\text{trans}_f * \text{trans}_g(t)}{r_w} v = \sigma_t(t) v \quad \text{(Equation 3)}$$

(A4) *Engine speed for BEV powertrain*: In BEV, which typically have a single gear, σ_{BEV} is constant. Neglecting tire slip, the engine speed of BEV (N_{BEV}) becomes proportional to the vehicle speed and can be expressed by Equation (4).

$$N_{BEV} = \sigma_{BEV} v_{sect} \quad \text{(Equation 4)}$$

(A5) *Engine speed for ICEV powertrain*: For ICEV, $\text{trans}_g(t)$ varies based on the engaged gear:

(A5a) In urban areas, gear shifts maintain a steady engine speed modeled by Equation (5), where N_e represents the typical urban engine speed recommended for the engine, adjusted by the driver aggressiveness factor μ_N.

$$N_u = \mu_N N_e \quad \text{(Equation 5)}$$

(A5b) In rural areas (countryside and highway), the highest gear is assumed to remain engaged, making the engine speed proportional to vehicle speed and dependent solely on the gearbox ratio σ_f as shown by Equation (6).

$$N_r = \sigma_f v_{sect} \quad \text{(Equation 6)}$$

(A5c) During acceleration, engine speed N_a is considered constant. This parameter depends on the driver behavior.

These assumptions result in rectangular functions for the *target engine speed functions* (when neglecting acceleration, braking and driver influence during cruising). The impact of the driver on the *real engine speed* depends on the type of powertrain. These *real engine speed functions* are illustrated in Figure (2b).

Third, power demand equations require integration of the squares of the torque T^2 for core losses, and of the power demand P_{in}^2 for battery losses. Yet, these variables are non-linear. The torque (T) is defined as a function of the engine speed (N) and the power supplied by the engine (P_{out}) as shown by Equation (7) [36]. Assumption A6 provides further simplifications for modeling these dynamic variables.

$$T = \frac{P_{out}}{N} \quad \text{(Equation 7)}$$

(A6) *Squared Torque and Power*: According to the literature, torque is significant during acceleration phases but negligible during cruising [38,79]. Equation (8) simplifies the squared torque setting it equal to the squared torque at acceleration (T_a^2). Moreover, power demand differentiates between cruising and acceleration, following Equation (9) to account for substantial power demands during acceleration (P_a^2) compared to cruising ($\widetilde{P}_{cruise}$) which is averaged, obtaining a rectangular *target function* [38,79].

$$T^2(t) = T_a^2 = \left(\frac{\mu_a P_{max}}{N_a}\right)^2 \quad \text{(Equation 8)}$$

$$P^2(t) = P_a^2 + (\widetilde{P}_{cruise})^2 \quad \text{(Equation 9)}$$

Fourth, assumption A7 simplifies the modeling of the road slope and wind speed as a function of the path.

(A7) *Slope and Wind:* The model accounts for the average road slope and wind speed impacting the vehicle in each section.

In summary, this model introduces specific parameters characterizing independently the path and the driver behavior. The *target functions,* which represent the impact of the path on dynamic parameters, are all rectangular functions. The *real functions* are adapted from these target functions to represent the driver influence during acceleration, braking and cruising phases.

2 Parametrized integration of driving conditions

The integration of dynamic variables follows a two-step approach: first, the target functions are integrated to compute parameters characterizing the path. Then adjustments are made to integrate the *real function*, to characterize the influence of the driver behavior.

Since target functions are rectangular, they can be integrated manually by weighting the dynamic parameter values by the length of each segment. For real function integration, separate calculations are performed for cruising, acceleration, and deceleration. The proportion of these phases over the total distance depends on the frequency, on the intensity of incidents along the path, and on the driver behavior. During cruising, the real functions are easily integrable as they are constant and proportional to the target functions. For braking, significant differences exist between ICEVs and BEVs. In ICEVs, braking does not consume power supposing the clutch is always engaged, so braking phases are excluded from the integration bounds. In BEVs, regenerative braking recovers inertia power. Losses are included in the integrals to account for energy dissipated by external forces and unrecovered powertrain losses. For acceleration of all automobiles and for braking of a BEV, a

ratio r_{acc} is introduced, representing the ratio of average speed during acceleration to the final cruising speed. This ratio depends on the incident along the path and adjusts the integration to account for speed reductions during these phases.

Energy consumption equations, derived from this methodology, are compiled in **Supplementary Information SI-1.**

3.1.3. Generalization of the PIEC and specific calculation of the MIEC

This work generalizes the concepts of Fuel Reduction Value (FRV) and Mass Induced Fuel (MIF) introduced by Eberle et al. (1998) [82] and Kim et al. (2013) [34] respectively. These parameters, used to assess automobile lightweighting, quantify the reduction in automobile energy consumption achieved per kilogram of mass reduction, typically expressed in l/100km/100 kg. It is proposed that for any parameter P of the model, the PIEC can be derived from the energy consumption equations for any automobile (both GV and BEV) as expressed in Equation (10).

$$PIEC = \frac{dEC}{dP} \ (Eq.\ 10) \qquad \text{(Equation 10)}$$

As an example, the Mass Influence on the Energy Consumption (MIEC) is derived from the parametrized model to obtain an analytical expression applicable to both ICEVs and BEVs, which is calculated in Equation (11).

$$MIEC = \frac{dEC}{dM} = \frac{10}{3.6} \cdot \frac{1}{\eta_{i,e}\eta_{i,dr}\eta_{i,bat}} \left(r_0 g J_1 + \left(1 - \eta_{regen}\right) K_1 + g\mathscr{K}\right) \qquad \text{(Equation 11)}$$

where $\eta_{i,e}, \eta_{i,dr}, \eta_{i,bat}, \eta_{regen}$ are the indicated efficiencies of the engine, the drivetrain, the battery and the regenerative braking; $r_0[-]$ is the rolling factor; g [m/s^2] is the acceleration gravity; $J_1\ [-], K_1\left[m/s^2\right], \mathscr{K}\ [-]$ are the dynamic variable integrals of the speed, the inertia and the slope.

Although Kim assumed that all powertrain losses are directly dependent on mass, our model showed that the MIEC is only dependent on indicated efficiencies. However, a lower mass can induce additional reductions of consumption such as engine downsizing or gear ratio adjustments. These can be included as potential secondary reductions in the analysis. An additional $MIEC_{SR}$ can been calculated considering a gear ratio (σ_f) reduction proportional to the mass reduction (Equation (12)).

$$MIEC_{SR} = \frac{\sigma_f}{M}.\sigma_f IEC \qquad \text{(Equation 12)}$$

3.2. Data acquisition and preparation for validation and pre-set configurations generation

This section outlines the methodology for data acquisition and preparation. The collected data quantify parameters describing automobile body, powertrain elements, path, and driver behavior, supporting the validation of the physics-based models developed and the creation of pre-set configurations.

3.2.1. Data collection methodology to validate the physics-based model

For model validation, empirical data from manufacturers' legal vehicle tests, which measure energy consumption using specific driving cycles, were collected. Validation involved reproducing these tests using the parameterized model and comparing the empirical results with simulations. The model's parameters were set with data characterizing the specific automobile, engine, and driving cycles associated with each test.

Efficiency maps derived from test benches for gasoline engines, electric engines, and transmission were obtained from the United States Environmental Protection Agency (EPA) [83–86]. Optimized values of the parameters were determined within a realistic range guided by literature to minimize the relative errors between our model and the empirical efficiency map for the most representative operating conditions for automobile [36,87] ($\tilde{N}$ [1000 rpm–4000 rpm] and T ~ [0-0.5T_{max}]). Details of this process are available in **Supplementary Information SI-3A**. In total, eighteen gasoline engines, five electric engines, and three transmission types were tested. Additionally, synchronization losses in gearboxes were quantified from Habermehl et al. [74].

Characteristics of automobiles equipped with engines with efficiency maps available in the EPA database were collected from manufacturer databases or catalogs [69,88–91]. Overall, twenty GV and eight BEV were modeled for validation.

Key parameters introduced in the parametrized integration method were quantified from driving cycles. Cruise speed, acceleration, and deceleration related parameters were extracted by analyzing speed variation as documented in **Supplementary Information SI-3B.** Average engine speeds during cycles were estimated from literature references [36,87], alongside data on accessories or payloads imposed by test regulations [60,92]. Overall, seven driving cycles were tested: WLTP and NEDC (Europe), JC08 (Japan), and EPA-FTP75, HWFET, US06, and SC03 (USA). Some cycles included sub-cycles to represent specific driving conditions.

Finally, the energy consumption results of these automobiles across various driving cycles were collected from specialized agencies. By quantifying the parametrized model with the collected data, simulations were conducted, and their results were compared to empirical tests.

3.2.2. Data collection methodology to produce pre-set configurations

Multiple existing databases that characterize and categorize automobile bodies were compiled and compared [25,36,93–96]. These databases encompass various automobile technologies, typically classified by size. However, segmentation and/or nomenclature differ across inventories due to regional standards. This paper proposes a unified classification system with six size categories: mini, compact, medium, large, SUV, and pick-up. No complete datasets for specific regions or countries were found in the literature. Such reference inventories were compiled for the United States, Quebec, the European Union, and the United Kingdom. These inventories are based on the distribution of the six automobile categories within regional automobile markets, derived from national agency studies [97–100].

Technical papers on the efficiencies of gasoline engines [33,49,65,101–104], electric engines [25,48,90,96,103,105,106], drivetrains [73,74,107–111], and batteries [75–79,96] were reviewed to estimate average mean displacement and mean power of the powertrain for US [98] and EU [100]. This enabled the computation of preset configurations for different technologies and average automobile sizes by region.

Finally, average travel patterns were derived from regional driving cycles to quantify path parameters. Road slope and wind parameters were incorporated using literature datasets [92]. Given that driver aggressiveness is often underestimated in driving cycles, additional data from the literature was also used to model deceleration behaviors [112–114], acceleration aggressiveness [115], and speed compliance [116–118].

Following this method, pre-set configurations were built for each contributor: 10 car body configurations, 6 gasoline engines, 6 electric engines, 9 drivetrains, 9 paths, and 7 driver behaviors. The main parameters introduced in the model are quantified in Table 1 for four of these configurations per contributor (two technical scenarios and two regional averages). All other parameters are available in **Supplementary Information SI-2**.

Table 1
Main parameters characterizing the contributors to automobile energy consumption. Parameters are evaluated for various pre-set configurations.

Contributor	Pre-set configurations			
	Technical Scenarios		Regional Scenarios	
Car Body	**Compact**	**SUV**	**Average EU**	**Average US**
M_{car} [kg]	1233	1877	1570	1869
r_0 [−]	0.009			
C_d [−]	0.40	0.46	0.43	0.47
A [m^2]	2.21	2.89	2.52	2.87
P_{acc} [kW]	350	500	440	475
$\boldsymbol{r_0}$ [−] rolling factor; $\mathbf{M_{car}}$ [kg] vehicle weight (including accessories); $\boldsymbol{\rho}$ [−] air density; $\boldsymbol{C_d}$ [−] drag coefficient (including accessories); **A** [m^2] vehicle frontal area; $\boldsymbol{P_{acc}}$ [W] average power of accessories;				
Gasoline Engine	**Small (EU)**	**Large (EU)**	**Average EU**	**Average US**
D [L]	1.3	2.3	1.6	2.8
$\eta_{d,GV}$[−]	0.43			
D [L] engine displacement; $\boldsymbol{\eta_{d,BEV}}$ [−] differential efficiency of the BEV.				
Electric Engine	**Small**	**Large**	**Average EU**	**Average US**
P_e [kW]	60	300	169	190
$\eta_{d,BEV}$ [−]	0.98			
$\boldsymbol{P_e}$ [kW] maximum power of the engine; $\boldsymbol{\eta_{d,BEV}}$ [−] differential efficiency of the BEV.				
Drivetrain (GV)	**Manual - FWD**	**Auto - AWD**	**Average EU**	**Average US**
$\eta_{d,dr}$ [−]	0.97	0.93	0.96	0.94
a_{tr} [10^{-5} s]	2.1	4.0	2.7	3.6
Drivetrain (BEV)	**Auto - FWD**	**Auto - AWD**	**Average EU**	**Average US**
$\eta_{d,dr}$ [−]	1	0.97	0.99	0.98
a_{tr} [10^{-5} s]	0	1.0	0.2	0.6
$\boldsymbol{\eta_{d,dr}}$ [−] differential efficiency of the drivetrain; $\boldsymbol{a_{tr}}$ [s] drivetrain frictions characteristic coefficient.				
Battery	**Worst**	**Best**	**Average World**	
$\eta_{d,bat}$ [−]	0.85	0.95	0,9	
R [ohm]	0.4	0.3	0.35	
U [V]	400	350	375	
$\boldsymbol{\eta_{d,bat}}$ [−] differential efficiency of the battery; **R** [ohm] internal resistance of the battery; **U** [V] battery voltage;				
Path	**City (Mean)**	**Highway (EU)**	**Average EU**	**Average US**
$\mathscr{J}_{3,p}[m^2/s^2]$	134	1155	616	460
$\mathscr{K}_{1,p}[m/s^2]$	0.20	0.01	0.14	0.13
r_{urban}[−]	1	0	0.5	0.4
h[−]	0.002			
$\boldsymbol{\mathscr{K}_{1,p}}$ $[m/s^2]$, $\boldsymbol{\mathscr{J}_{3,p}}[m^2/s^2]$ *and* $\boldsymbol{h}$ [−] integrals of the dynamic parameters related resp. to the inertia, the drag, and the slope, along the target function (which only depends on the path). $\boldsymbol{r_{urban}}$[−] share of the journey traveled in urban area.				
Driver	**Eco-driver**	**Aggressive**	**Average EU**	**Average US**
B [m/s^2]	0.55	1.06	0.72	0.72
μ_v [−]	0.90	1.10	0.98	1.08
μ_a [−]	0.05	0.10	0.08	0.05
$\boldsymbol{\mu_v}$ [−] Driver speed compliance ratio; $\boldsymbol{B}$ [m/s^2] mean deceleration by the driver during braking; $\boldsymbol{\mu_a}$ [−] Driver acceleration aggressiveness.				

3.3. Energy consumption computation tool and case study selection

3.3.1. PETRAUL – the parametrized energy tool for representativeness of automobile in LCA

An energy consumption calculation tool that computes the final equations and the pre-set configurations was developed. *PETRAUL*[1] [119] enables practitioners to generate specific energy consumption results using pre-set configurations, or by quantifying the model's parameters with finer or more specific datasets they have compiled. This flexibility ensures the tool's usability across various scenarios. The tool's output includes the energy consumption for a specified scenario and a contribution analysis that quantifies the energy losses attributable to the different contributors. It also includes the calculation of the PIEC of the most contributive parameters of the model, for the specific scenario modeled by an LCA practitioner.

3.3.2. Presentation and preparation of the applications

Three case studies were developed to exemplify the tool's functionality. These cases demonstrate how *PETRAUL* operates, highlight its advantages compared to existing inventories such as *ecoinvent*, and showcase its wide range of potential applications.

1 Scenario analysis

First, an analysis of the sensitivity of energy consumption to the main contributors was performed using *PETRAUL*. The European average scenario, representing average technology, path, and driver, was selected as the reference scenario. Alternative scenarios were generated by systematically varying the configuration of one contributor at a time. Four scenarios were tested for the following contributors: the car body (mini, compact, SUV, pick-ups), the engine (Very small, Small, Large, Very Large), the path (Average City, Dense City, Highway, Countryside), and the driver behavior (Extra Ecodriving, Ecodriving, Aggressive, Extra Aggressive).

2 Comparison with ecoinvent and Carculator

Second, a comparison was performed between PETRAUL model, Carculator, and *ecoinvent*. *ecoinvent* defines three categories of GV based on mass: small (<1400 kg), medium (≈ 1600 kg) and large (>1800 kg). For BEV, *ecoinvent* offers only one average automobile category. *PETRAUL* and Carculator propose several technical configurations per ecoinvent category. For each category, the average energy consumption of automobiles in this category was estimated for Carculator, while a distinction between US average and Europe average was performed for PETRAUL. Additionally, best-case and worst-case estimates with PETRAUL and Carculator were computed for each category, capturing the range of possible energy consumption that actually exists within the defined ecoinvent categories due to variability in technology design and driving conditions.

3 Application to lightweighting

Third, a streamlined LCA approach of automotive lightweighting is developed to demonstrate how the parametrized model enhances regional and technological correlation in foreground LCA modeling. While lightweight materials reduce energy consumption throughout the automobile's use phase, they can increase production impacts [120–125], potentially shifting the environmental burden to manufacturing. This analysis calculates the maximum additional manufacturing costs of a lightweight component to remain advantageous for Climate Change depending on technological and regional contexts. This analysis is inspired by the method developed by Kelly et al. (2021) [125].

For the production phase, traditional (t) and lightweight (l) components are characterized by their carbon intensity of production per kilogram of material produced i_{prod} $\left[kgCO_2eq./kg_{prod}\right]$ and the substitution factor f [−] which corresponds to the mass ratio between two materials required to achieve functional equivalence when replacing one material with another. For the use phase, inputs include the mass reduction induced by the shift to the lightweight material ΔM $\left[kg_{red}\right]$, the lifetime d $[km]$, the MIEC $\left[kWh/100km/100kg_{red}\right]$, and the carbon intensity of the energy source (i_{energy}). Moreover, the use phase also in-

[1] PETRAUL tool can be found at https://petraul.streamlit.app/.

cludes additional emissions proportional to automobile mass, such as exhaust and infrastructure. $e\left[kgCO_2/(kg_{red}.km)\right]$ represents the intensity of these emissions. The climate change impact score's difference ΔCC between traditional and lightweight components is expressed by Equation (13).

$$\Delta CC = \left(\frac{i_{prod,t} - i_{prod,l}.f}{1-f}\right)\Delta M + \left(MIEC.i_{energy} + e\right)\Delta M.d \qquad \text{(Equation 13)}$$

Lightweight material performs better than traditional material for climate change when the increase of the manufacturing impact score (the first term of equation (11)) is lower than the benefits of the use phase (the second term of equation (11)). In other words, the breakeven additional manufacturing costs per kg of mass reduction ($\Delta I_{prod,breakeven}$), indicating the maximum increase of $\left(\frac{i_{prod,t}-i_{prod,l}.f}{1-f}\right)$ for the lightweight system to remain beneficial for climate change, is obtained in Equation (14) by setting $\Delta CC = 0$ in Equation (13).

$$\Delta I_{prod,breakeven} = \left(MIEC.I_{energy} + e\right).d \qquad \text{(Equation 14)}$$

The case study of an innovative lightweight glazing for automobile was performed to illustrate this approach. The replacement of traditional tempered glass glazing ($i_{prod,g} = 1.25\ kgCO_2eq./kg_{prod}$) with polycarbonate (PC) lightweight glazing prepared by injection molding ($i_{prod,PC} = 7.03\ kgCO_2eq./kg_{prod}$) was assessed. The PC has a density of 1200 kg/m^3 and requires 4.5 mm of thickness while glass has a 2500 kg/m^3 density and requires 3.25 mm of thickness, leading to a substitution factor of $f = 0.66$. The lifetime of both glazings was assumed equal to the lifetime of the automobile: $d = 150,000km$. Additional details on production modeling can be found in **Supplementary Information SI-4**.

For the use phase, the *MIEC* was computed using the parametrized model implemented in *PETRAUL* for eight driving scenarios (European Average, American Average, European Small automobile, and European average city driving conditions, all assessed for both GV and BEV). Following Koffler et al. (2010) [37], the secondary reductions were excluded from the case study boundaries since the mass reduction from lightweight glazing is not significant enough to justify them. However, $MIEC_{SR}$ was calculated to assess the sensitivity of the MIEC to secondary reduction.

Exhaust emissions were quantified to $e = 0.061 kgCO_2/100km/100kg_{red}$ using *ecoinvent*. Four regions—Swiss (CH), Rest of Europe (RER), United States (US), and Quebec (QC)—were considered for the energy source intensity during the use phase. The carbon intensity of petrol was assumed to be constant globally, with $i_{petrol} = 362\ gCO_2eq./kWh$. The carbon intensity of the electricity mix was regionalized with *ecoinvent*: $i_{RER} = 328\ gCO_2eq./kWh$, $i_{CH} = 33 gCO_2eq./kWh$, $i_{US} = 479\ gCO_2eq./kWh$ and $i_{QC} = 14\ gCO_2eq./\ kWh$.

4. Results

4.1. Model validation

As a first step of validation, the powertrain loss models were validated using efficiency maps available from the EPA [83]. Figure 3 exemplifies this validation process. It shows the relative error across 110 representative operation points for a Mazda 2.5L Tier 2 gasoline engine. These points reflect the difference between the empirical map values and our model quantified with optimized parameters. The average relative error for the selected operation points equals 0.99 %. This process can be replicated for other powertrain elements using the Jupyter notebook provided in **Supplementary Information SI-3A**. The models proposed in this paper demonstrate strong consistency with empirical efficiency maps for all tested powertrain elements. The calculated average relative errors are 1.6 % for gasoline engines, 1.2 % for electric engines, and 2.1 % for transmissions.

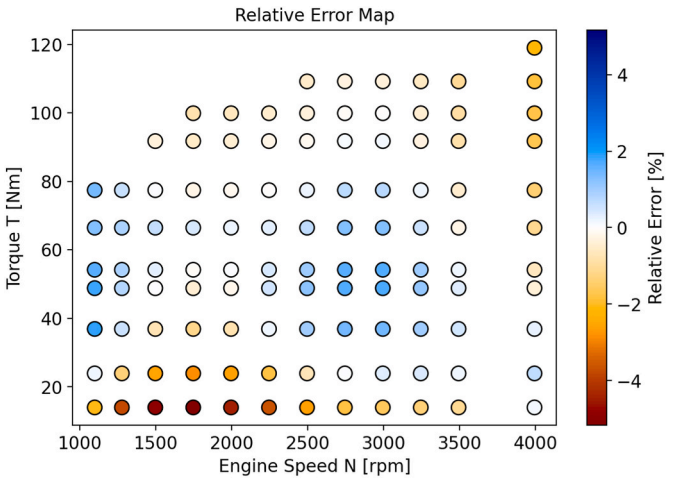

Figure 3. Relative Error Maps between the parametrized model and the empirical efficiency map for a Mazda 2.5l gasoline engine. The efficiency map is divided into 110 representative operating points, each colored based on the relative error: orange nuances indicate efficiency underestimated by the model, and blue nuances indicate efficiency overestimated by the model. (For interpretation of the references to color in this figure legend, the reader is referred to the Web version of this article.)

As a second step of validation, the complete energy consumption model was tested following the methodology presented above and computed in **Supplementary Information SI-3C**. Figure 4 displays the relative error distribution between manufacturer-provided data and model simulations for different categories of tests. Overall, the models are in good agreement with the manufacturer tests, with deviations reaching a maximum of ±10 %. Furthermore, the distributions reveal no evidence of systematic errors, as relative errors for all categories are evenly scattered around 0 %.

4.2. Illustrative applications of PETRAUL for environmental assessment

In this section, the results obtained with *PETRAUL* and computed in **Supplementary Information SI-3D,** are presented and analyzed, illustrating the tool's ability to provide detailed and adaptable insights into a large range of environmental impact assessment applications.

4.2.1. Scenario analysis: identification of potential for energy consumption reduction

The fuel consumption across the average European GV and twenty alternative scenarios were generated with *PETRAUL*, with results shown in Figure 5. The average fuel consumption for a European GV is calculated at 7.16 l/100 km, closely matching the real-world average value of 7.33 l/100 km reported by EEA [90] in 2024. The graphs reveal that larger automobiles, more powerful engines, and aggressive driving styles significantly increase energy consumption. Urban driving is identified as the least efficient scenario due to elevated inertia power demands and high engine friction losses, which are further exacerbated by traffic conditions. A detailed analysis reveals comparable energy reduction potential across improvements in the car body, the engine, and driving behavior. Incremental improvements within a category can reduce consumption by 6–14 %, while optimal configuration within a category achieves reductions of 16–22 %. Transmission types and driveline architectures are less contributive, with optimal drivetrain configuration reducing the consumption by around 5 %. While these contributions are significant enough to warrant industrial attention, they are insufficient as standalone solutions. These findings emphasize the necessity to integrate multiple solutions and to couple efforts across all contributors to achieve meaningful reductions in energy consumption.

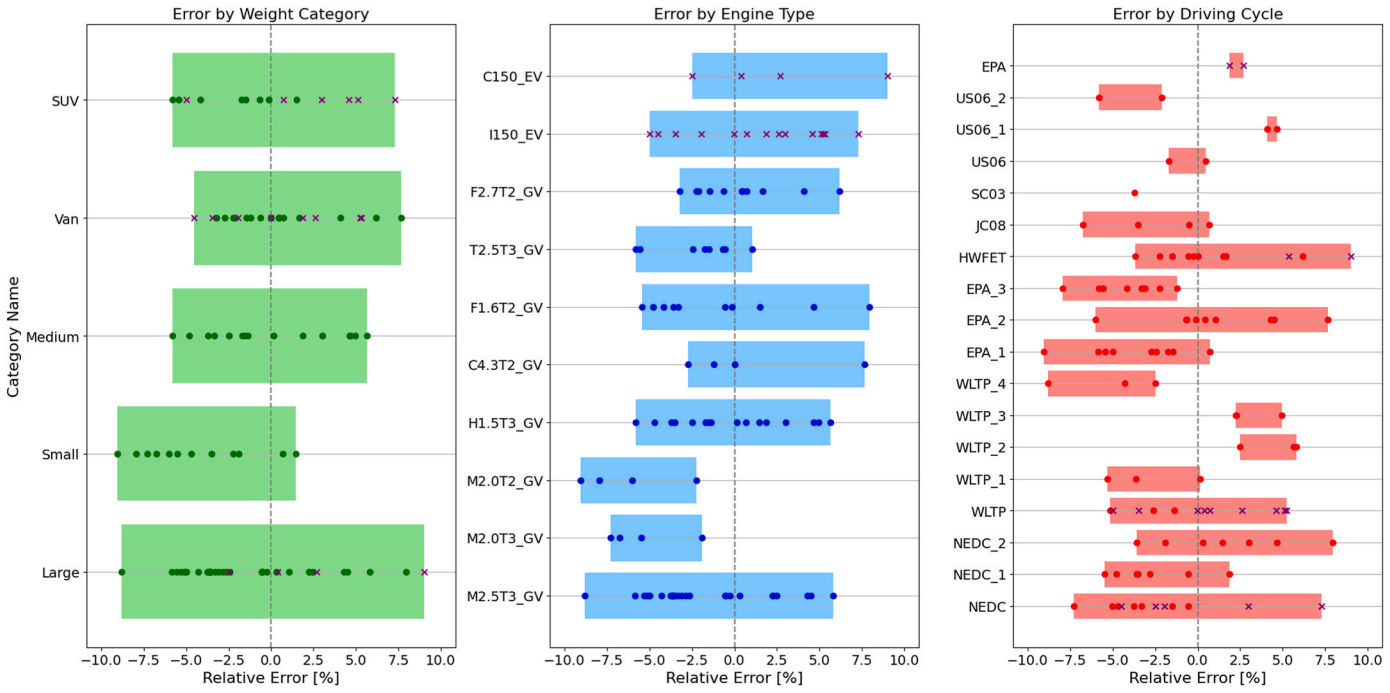

Figure 4. Distribution of the relative error between parametrized model and manufacturer empirical energy consumption measurements. Each point (for GV) and cross (for BEV) represents a single simulation. Shaded regions indicate the range of relative errors for each category. Simulations are classified by:
(a) car body weight categories;
(b) the engine type, with the engine naming convention (e.g., M2.5T2_GV) referring to the Constructor Initial (e.g., M for Mazda)- the Engine Displacement(L) for gasoline engines or Engine Power(kW) for electric engines-the Emission Standards for gasoline engine (Tier2 or 3)-the fuel type (gasoline or electric);
and (c) driving cycles (e.g., WLTP, NEDC) or portion of driving cycle (WLTP_1, WLTP_2).

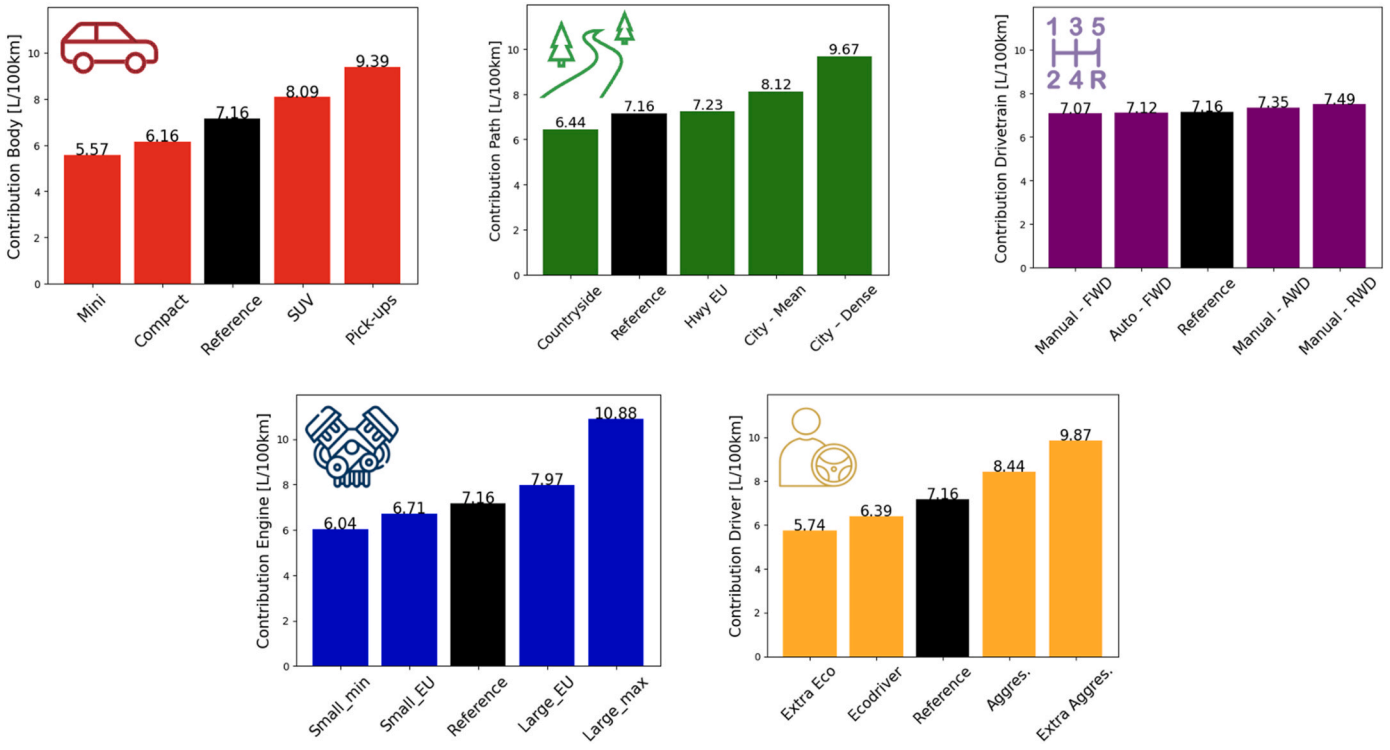

Figure 5. Computation of energy consumption for twenty-one GV pre-set configurations. The average European GV is shown as the reference. Alternative scenarios, which vary one contributor at a time, are classified by the contributor affected: the body (red), the engine (blue), the path (green), the driver (yellow), and the drivetrain (purple). (For interpretation of the references to color in this figure legend, the reader is referred to the Web version of this article.)

4.2.2. Improvement of aggregated car processes representativeness and granularity: comparison with ecoinvent and Carculator

Energy consumption results of the PETRAUL model are compared with *ecoinvent* and Carculator in Figure 6. For instance, when modeling in an LCA the energy consumption of a medium gasoline car as defined by ecoinvent (1400–1800 kg), ecoinvent considers one unique category (1600 kg) consuming 8.36L/100 km (green dot). Carculator proposes three configurations of vehicles in this category (Compact, Midsize, and Midsize SUV) and two driving cycles (NEDC, WLTP), ranging the energy consumption between 5 and 7.8 l/100 km (sky blue area), with an average configuration consuming 7l/100 km (blue star). PETRAUL offers more flexibility and adaptability by proposing hundreds of configurations in this 'Medium' category. Results range from 4.8l/100 km for the best-case scenario (lower medium car with a small engine, driven by an extra eco-driver mainly in a town with low traffic) to 15.1l/100 km for the worst-case scenario (SUV with a powerful engine, driven by an extra aggressive driver in traffic). This range is represented by the gray area. PETRAUL also provides averages for the European context (7.2l/100 km) and the American context (9.7l/100 km). This regional difference is driven by vehicle and powertrain sizing as well as driving conditions, and is more pronounced for larger vehicles and for GV compared to BEV.

This figure demonstrates that while *ecoinvent*'s modeling is relatively consistent in reflecting average real-life technologies and driving conditions, it underestimates energy consumption for American automobiles and overestimates it for European cars due to a lack of a finer regional resolution in the modeling. Moreover, the comparison between ecoinvent single point with PETRAUL and Carculator ranges illustrates the high uncertainty in *ecoinvent*'s model and underscores the database's limited resolution in capturing diverse driving conditions. Carculator model shows more flexibility by introducing various technical scenarios. Yet, the modeling of driving conditions with driving cycles leads to an underestimation of energy consumption for all categories of vehicles. Additionally, Carculator does not provide regional pre-set configurations to distinguish American and European cars. Overall, this figure highlights that the finer resolution proposed by PETRAUL increases the technological and regional representativeness of the automobile process in LCA.

4.2.3. Application to foreground modeling: is a lightweight polymer glazing relevant?

The parametrized model was applied to calculate the MIEC, which ranges from 1.5 to 1.8 kWh/100km/100kg_{red} for GV (i.e., 0.17–0.20 l/100km/100kg_{red}) and 0.4–0.45 kWh/100km/100kg_{red} for BEV, as represented in Figure 7a. These values increase to 2.4–3.4 kWh/100km/100kg_{red} (i.e., 0.27–0.38 l/100km/100kg_{red}) and 0.45–0.55 kWh/100km/100kg_{red}, respectively, when accounting for gear ratio adjustment as a secondary reduction. While the MIEC remains consistent across automobile and engine sizes, it increases significantly for GV in city driving, whereas BEVs exhibit near-constant values across scenarios. Contextualized benefits of lightweighting materials during use phase were derived from MIEC results (Figure 7b). For GV, the benefits are estimated at 10–12 $kgCO_2eq./kg_{red}$. The benefits for BEV show high sensitivity to electricity grids, with values of 1.7–1.8 $kgCO_2eq./kg_{red}$ in low-carbon regions like Switzerland and Quebec, almost doubling in the European mix (3.3 $kgCO_2eq./kg_{red}$) and rising 2.5 times in the U.S. mix (4.1 $kgCO_2eq./kg_{red}$).

When considering the replacement of traditional glass glazing with PC glazing, the additional manufacturing cost is calculated to be 10.2 $kgCO_2eq./kg_{red}$. This additional cost is compared with the contextualized benefits of the PC glazing during use phase (Figure 7b). Lightweight PC glazing negatively impacts the climate change score for BEV, as the

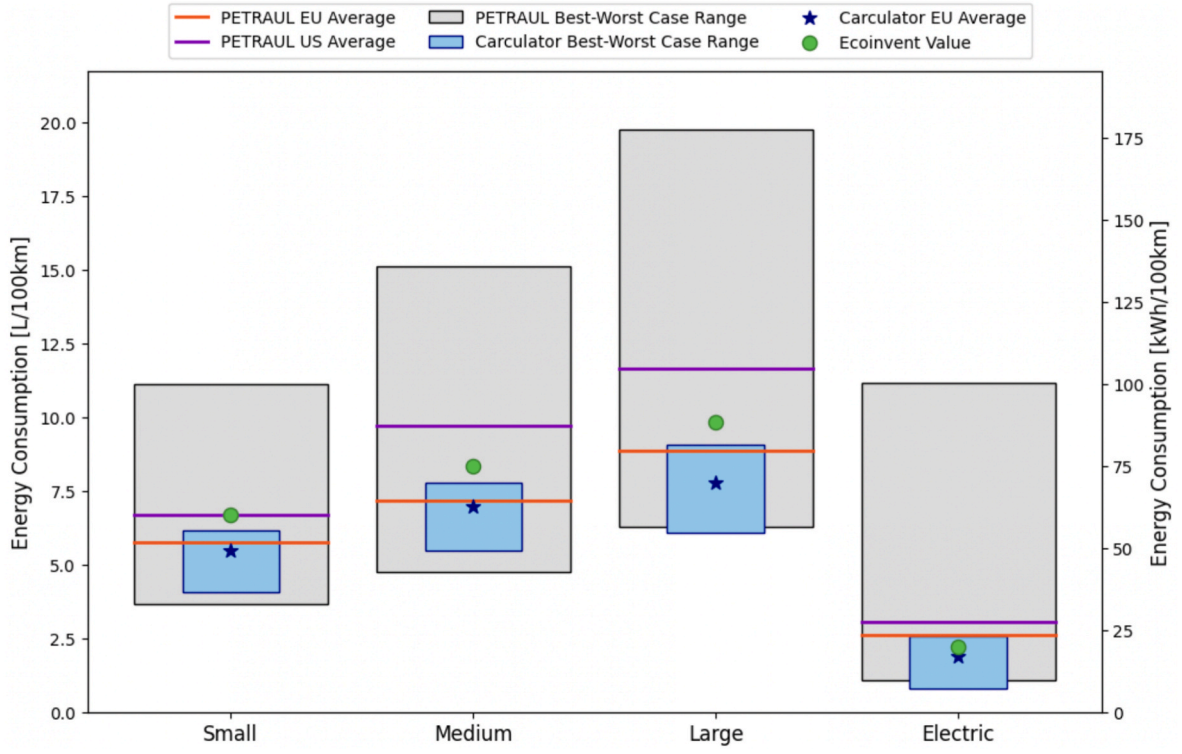

Figure 6. Comparison between PETRAUL, Carculator, and ecoinvent for the four categories of automobile modeled in ecoinvent. Green dots represent ecoinvent data. PETRAUL and Carculator capture greater variation in technologies and driving conditions, resulting in a broader range of possible energy consumption within each category. This range of results obtained with Carculator is represented for each category by a sky-blue area, and the average Carculator configuration is highlighted by a blue star. Colored lines correspond to PETRAUL results for European (blue) and American (red) average configurations. Gray areas represent the range of energy consumption obtained with PETRAUL within the categories. The conversion factor from liters of fuel to kWh is the lower heating value (LHV) of gasoline (LHV = 8.9 kWh/l). (For interpretation of the references to color in this figure legend, the reader is referred to the Web version of this article.)

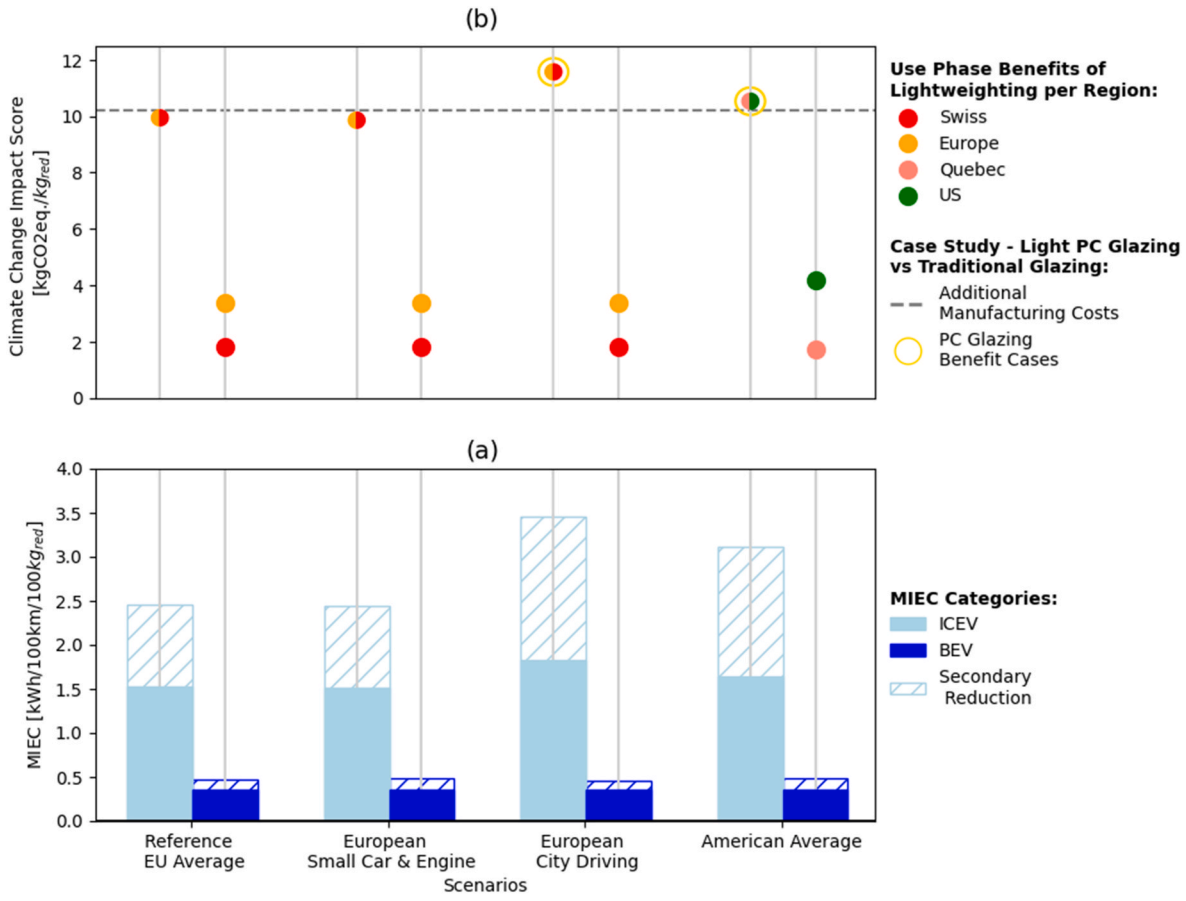

Figure 7. Results of the MIEC calculation and of the streamlined LCA of the lightweight PC glazing case study for different technologies, driving conditions, and regions. (a) MIEC is calculated for four driving scenarios and represented with bars (light blue for GV, dark blue for BEV). Hashed areas indicating the gear ratio adjustment secondary reduction (excluded from the case study scope). (b) Streamlined LCA results. Colored points mark the use phase benefits of lightweight materials depending on the context (technology and region). For the case study (PC glazing), this manufacturing additional cost is plotted as a gray dashed line. Only the points above this threshold line (circled in yellow) provide a carbon benefit over the life cycle of the car when substituting glass with PC glazing. (For interpretation of the references to color in this figure legend, the reader is referred to the Web version of this article.)

production-phase emissions outweigh the use-phase benefits across all scenarios. For GV, the results vary based on driving conditions and the region studied. In the European context, traditional glazing performs slightly better under average driving conditions, but specific scenarios, such as 100 % city driving, reverse this trend. For the average American automobile, PC glazing is also more favorable. The results presented in Figure 7b can be extrapolated to obtain total climate change results. PC glazing achieves a weight reduction of approximately 10 kg for the entire automobile (**SI-4**). As read in Figure 7b, in the European GV context, PC glazing increases the carbon score of the automobile by 0.2 $kgCO_2eq./kg_{red}$ (manufacturing additional costs of 10.2 $kgCO_2eq./kg_{red}$ minus use phase benefits of 10.0 $kgCO_2eq./kg_{red}$) while it reduces these emissions by 0.3 $kgCO_2eq./kg_{red}$ in the American GV context. These results translate into an increase of 2 $kgCO_2eq.$ over the vehicle's lifetime for the European scenario and a saving of 3 $kgCO_2eq.$ in the American GV context.

Additionally, the two glazing systems have been compared with other impact categories provided by Impact World + v2.0 [126]. The results for the Human Health and Ecosystem Quality categories, presented in **Supplementary Information SI-4**, are consistent with the carbon score for all scenarios.

Consequently, the analysis suggests that lightweight PC glazing should be avoided in BEV when aiming to reduce potential environmental impacts. For GV, given the close results between glazing options, and their high sensitivity to uncertain parameters like the glazing thickness, a complete LCA complemented by sensitivity analyses and Monte Carlo simulations would be necessary to determine the most appropriate strategy.

5. Discussion, limitations, and future work

5.1. Discussion

A parametrized model for automobile energy consumption was successfully developed in this study, uncoupling the contributors (automobile body, powertrain, path, and driver behavior). This approach enhances the transparency and robustness of environmental assessments by capturing the complex interplay between multiple variables. The inclusion of pre-set configurations in the tool facilitates model access for practitioners with varying expertise and resources by bridging data gaps that may hinder analysis.

The benefits of the parametrized model are illustrated through several applications. First, the model enables a detailed evaluation of the role of individual contributors in reducing energy consumption. Second, the high adaptability of the model significantly enhances background automobile process technological and regional representativeness compared to generic databases like *ecoinvent* or specific LCA models like Carculator. This enhanced representativeness holds significant potential for LCA. For instance, it can contribute to more accurate results for optimizing company and ride-hailing fleets, or for modeling activities requiring specific vehicles (e.g. pick-ups/utility vehicles for trade-related processes) or specific driving behavior (e.g. last-mile driving in

delivery processes). The parametrization of the process also facilitates the update of the datasets, and allows an easier integration of new technological innovations in the database. Third, the model proves valuable for foreground LCA modeling. The generalization of the PIEC enables to capture use phase benefits of any innovation influencing the energy consumption of a car. The streamlined LCA model for assessing the relevance of lightweight materials in automobiles exemplifies how the PIEC can be integrated into LCA, enabling the generation of context-specific results with greater transparency, adaptability, and reproducibility. This is demonstrated through the assessment of the lightweight PC glazing, where LCA results provide contrary conclusions depending on the technology (typically GV or BEV), the driving conditions, and the geographical context. This adaptability ensures that the model captures nuanced trade-offs across varying conditions and materials, providing actionable insights for decision-making.

Overall, these applications support the need to move beyond purely techno-oriented solutions to reducing the environmental impacts of mobility. They highlight the need for multi-solution strategies, emphasizing that meaningful reductions require the involvement of all stakeholders, from manufacturers to drivers. The PC glazing case study challenges the broadly supported lightweighting policy within the automotive industry. It highlights the need to carefully assess the environmental impacts of any lightweight material, particularly as the electrification of automobiles continues to expand, reducing the MIEC of automobiles and, consequently, the maximum additional manufacturing costs allowed for lightweight systems to outperform traditional systems. Even when lightweight material seems beneficial, the net results must be carefully evaluated. PC glazing achieves a weight reduction of approximately 10 kg for the entire automobile, translating into a carbon savings of around 3 kg CO_2 equivalent over the vehicle's lifetime in the American GV context. This represents a mere 0.01 % reduction in the automobile's total carbon footprint. Moreover, the average weight of automobiles sold continues to increase due to upsizing, demonstrating that lightweighting alone is not a silver bullet for reducing the mass of automobiles [98]. Given these limitations, presenting these innovations as sustainable improvements could constitute greenwashing. Instead, they should be viewed as incremental progress that should be combined with alternative industrial and governmental policies such as electrification, downsizing, reducing travel distances by car, and promoting active mobility solutions.

5.2. Limitations and future works

However, the study also reveals some inherent limitations in the modeling approach. Developing a parametrized model demands a deep understanding of both the system under study and the mathematical frameworks used to accurately represent the physical process. For instance, the parametrization of powertrain-related energy losses involves complex nonlinear relationships, which are challenging to model precisely without extensive computational resources. To ensure usability and computational feasibility, certain simplifications were necessary for this study, such as omitting dependencies on variables like temperature, material aging, and instantaneous state-of-charge (SoC) for batteries. While these simplifications support model usability, they may compromise accuracy by not capturing specific factors that can influence energy consumption under real-world conditions. Given these challenges, future research should prioritize refining specific analytical relationships, particularly those pertaining to the powertrain, to further improve model accuracy.

The balance between model fidelity and usability is further complicated by the need for robust validation data. Although the model has been tested using mainly empirical datasets (efficiency maps, automobile characteristics, and driving cycles), these were supplemented by processed data from literature where specific values were not available in the test descriptions (typically for engine speed or equipment influences). Furthermore, the aggressiveness factors introduced in the parametrized integration model were also quantified based on literature, since testing agencies do not provide real-world measurements for such parameters. While all these assumptions and processed datasets have been carefully documented to limit bias and support a transparent uncertainty evaluation, the model would benefit from calibration using fully empirical measurements. Such efforts, however, require significant computational resources and access to detailed performance data, which is often restricted due to industrial confidentiality. Future research should focus on developing new methods to empirically assess the energy consumption of vehicles based on independent and precise measurements of car body and powertrain parameters, along with a systematic assessment of driving aggressiveness factors to better capture real-world variability in vehicle performance.

The first version of PETRAUL is exclusively dedicated to calculating the energy consumption of GV and BEV, limiting the scope of the tool. As the methodology is reproducible, future work can focus on adapting the physical equations and preparing new pre-set configurations to expand the tool's scope to alternative scenarios. The analysis can be extended to new powertrains like diesel, hybrid, and alternative fuels by replicating the approach taken for GV and BEV, requiring a detailed physical description of the powertrain components to determine specific losses and differential efficiencies. Expanding this methodology to other modes of transportation, such as trucks, buses, and motorcycles, is feasible, but it may require adjustments to both the physical equations and the modeling of driving conditions, particularly to account for the technical limitations of trucks. Emerging technologies such as autonomous driving can be modeled by generating new pre-set configurations for modeling driver behavior, while further research is needed to model the broader impacts of autonomous driving, such as changes in traffic patterns. Finally, future developments of the tool could aim to parametrize the entire life cycle of the automobile process, extending beyond the use phase to include vehicle production and end-of-life stages.

Additionally, there is significant potential to generalize parametrized practices in the LCA field. The methodology developed in this study, based on physical process description, uncoupling of contributors, and inclusion of pre-set configurations, could serve as a framework for building these parametrized models. While developing such models requires substantial resources, the long-term gains in terms of adaptability, precision, and collaborative potential justify this investment.

CRediT authorship contribution statement

Gabriel Magnaval: Conceptualization, Methodology, Software, Investigation, Data curation, Validation, Visualization, Writing – original draft. **Anne-Marie Boulay:** Supervision, Conceptualization, Methodology, Writing – review & editing, Funding acquisition, Resources.

Declaration of competing interest

The authors declare they have no known competing financial interests or personal relationships that could have appeared to influence the work reported in this paper.

Acknowledgments

The authors thank Sebastian Wolff and Georg Seitfudem for their valuable review of the paper. The authors thankfully acknowledge the financial support of the National Research Council Canada (grant number 969364). The authors remain solely responsible for the article.

Appendix A. Supplementary data

Supplementary data to this article can be found online at https://doi.org/10.1016/j.rser.2025.115716.

Data availability

Supplementary Information is accessible at 10.5281/zenodo.14874992 [119].

 The code, Jupyter Notebooks, and datasets used for computing PETRAUL, validating the model, and generating some of the pre-set configurations are available at: https://github.com/gabrielmagnaval/PETRAUL.git.

References

[1] IPCC. Emissions Trends and Drivers. IPCC : climate Change 2022 - mitigation of climate change. Cambridge University Press; 2022. p. 215–94. https://doi.org/10.1017/9781009157926.004.

[2] Orsato RJ, Wells P. The automobile industry & sustainability. J Clean Prod 2007;15:989–93. https://doi.org/10.1016/j.jclepro.2006.05.035.

[3] Simons A. Road transport: new life cycle inventories for fossil-fuelled passenger cars and non-exhaust emissions in ecoinvent v3. Int J Life Cycle Assess 2016;21:1299–313. https://doi.org/10.1007/s11367-013-0642-9.

[4] Bieker G. A global comparison of the life-cycle greenhouse gas emissions of combustion engine and electric passenger cars. Communications 2021;49(30). 847129-102. International Council of Clean Transportation (ICCT) White Paper No 07-2021.

[5] Oda H, Noguchi H, Fuse M. Review of life cycle assessment for automobiles: a meta-analysis-based approach. Renew Sustain Energy Rev 2022;159:112214. https://doi.org/10.1016/j.rser.2022.112214.

[6] Del Duce A, Gauch M, Althaus HJ. Electric passenger car transport and passenger car life cycle inventories in ecoinvent version 3. Int J Life Cycle Assess 2016;21:1314–26. https://doi.org/10.1007/s11367-014-0792-4.

[7] Kannangara M, Bensebaa F, Vasudev M. An adaptable life cycle greenhouse gas emissions assessment framework for electric, hybrid, fuel cell and conventional vehicles: effect of electricity mix, mileage, battery capacity and battery chemistry in the context of Canada. J Clean Prod 2021;317:128394. https://doi.org/10.1016/j.jclepro.2021.128394.

[8] Romero CA, Correa P, Ariza Echeverri EA, Vergara D. Strategies for reducing automobile fuel consumption. Appl Sci 2024;14:910. https://doi.org/10.3390/app14020910.

[9] Alzaghrini N, Milovanoff A, Roy R, Abdul-Manan AFN, McKechnie J, Posen ID, et al. Closing the GHG mitigation gap with measures targeting conventional gasoline light-duty vehicles – a scenario-based analysis of the U.S. fleet. Appl Energy 2024;359:122734. https://doi.org/10.1016/j.apenergy.2024.122734.

[10] Heywood J, MacKenzie D. On the road toward 2050: potential for substantial reductions in light-duty vehicle energy use and greenhouse gas emissions. 2015.

[11] Wernet G, Bauer C, Steubing B, Reinhard J, Moreno-Ruiz E, Weidema B. The ecoinvent database version 3 (part I): overview and methodology. Int J Life Cycle Assess 2016;21:1218–30. https://doi.org/10.1007/s11367-016-1087-8.

[12] Mielniczek A, Roux C, Jacquinod F. Benchmark of ecodesign LCA tools at neighborhood scale. LCM 2023 the 11th internationa lConference on life cycle management. 2023.

[13] Hung CR, Kishimoto P, Krey V, Strømman AH, Majeau-Bettez G. ECOPT2 : an adaptable life cycle assessment model for the environmentally constrained optimization of prospective technology transitions. J Ind Ecol 2022;26:1616–30. https://doi.org/10.1111/jiec.13331.

[14] von Drachenfels N, Husmann J, Khalid U, Cerdas F, Herrmann C. Life cycle assessment of the battery cell production: using a modular material and energy flow model to assess product and process innovations. Energy Technol 2023;11. https://doi.org/10.1002/ente.202200673.

[15] De Ceuster G, Van Herbruggen B, Logghe S, Proost S. TREMOVE. Report for European Commission, DG ENV, transport & Mobility Leuven and KU Leuven. 2004.

[16] Cooper JS, Noon M, Kahn E. Parameterization in life cycle assessment inventory data: review of current use and the representation of uncertainty. Int J Life Cycle Assess 2012;17:689–95. https://doi.org/10.1007/s11367-012-0411-1.

[17] Mueller KG, Lampérth MU, Kimura F. Parameterised inventories for life cycle assessment. Int J Life Cycle Assess 2004;9:227. https://doi.org/10.1007/BF02978598.

[18] Provost-Savard A, Legros R, Majeau-Bettez G. Parametrized regionalization of paper recycling life-cycle assessment. Waste Manag 2023;156:84–96. https://doi.org/10.1016/j.wasman.2022.11.018.

[19] Gibon T, Hahn Menacho Á. Parametric life cycle assessment of nuclear power for simplified models. Environ Sci Technol 2023. https://doi.org/10.1021/acs.est.3c03190.

[20] Hollberg Alexander. A parametric method for building design optimization based on Life Cycle Assessment. Universität Weimar; 2016.

[21] Niero M, Di Felice F, Ren J, Manzardo A, Scipioni A. How can a life cycle inventory parametric model streamline life cycle assessment in the wooden pallet sector? Int J Life Cycle Assess 2014;19:901–18. https://doi.org/10.1007/s11367-014-0705-6.

[22] Douziech M, Besseau R, Jolivet R, Shoai-Tehrani B, Bourmaud J, Busato G, et al. Life cycle assessment of prospective trajectories: a parametric approach for tailor-made inventories and its computational implementation. J Ind Ecol 2024;28:25–40. https://doi.org/10.1111/jiec.13432.

[23] Stephan A, Prideaux F, Crawford RH. EPiC grasshopper: a bottom-up parametric tool to quantify life cycle embodied environmental flows of buildings and infrastructure assets. Build Environ 2024;248:111077. https://doi.org/10.1016/j.buildenv.2023.111077.

[24] Fang L, Rosset Y, Sarrazin B, Lefranc P, Rio M. Parametric LCA model for power electronic ecodesign process: addressing MOSFET-Si and HEMT-GaN technological issues. IET Power Electron 2025;18. https://doi.org/10.1049/pel2.12844.

[25] Sacchi R, Bauer C, Cox B, Mutel C. When, where and how can the electrification of passenger cars reduce greenhouse gas emissions? Renew Sustain Energy Rev 2022;162. https://doi.org/10.1016/j.rser.2022.112475.

[26] Ospital L, Margni M, Boulay A-M. Development of a parametrized and regionalized life cycle inventory model for tire and road wear particles. https://doi.org/10.2139/ssrn.5127152; 2025.

[27] Parekh Ruchit, Trabucco Dario. Recent progress in integrating BIM and LCA for sustainable construction: a review. Int J Sci Res Arch 2024;13:907–32. https://doi.org/10.30574/ijsra.2024.13.1.1772.

[28] Bhat CG, Mukherjee A, Meijer JPR. Life cycle information models: parameterized linked data structures to facilitate the consistent use of life-cycle assessment in decision making. J Transport Eng, Part B: Pavements 2021;147. https://doi.org/10.1061/JPEODX.0000308.

[29] Ross SA, Cheah L. Uncertainty quantification in life cycle assessments: exploring distribution choice and greater data granularity to characterize product use. J Ind Ecol 2019;23:335–46. https://doi.org/10.1111/jiec.12742.

[30] Kerdlap P, Low JSC, Tan DZL, Yeo Z, Ramakrishna S. M3-IS-LCA: a methodology for multi-level life cycle environmental performance evaluation of industrial symbiosis networks. Resour Conserv Recycl 2020;161:104963. https://doi.org/10.1016/j.resconrec.2020.104963.

[31] Mayer M, Bechthold M. Data granularity for life cycle modelling at an urban scale. Archit Sci Rev 2020;63:351–60. https://doi.org/10.1080/00038628.2019.1689914.

[32] [a]Sibiude G, Mailhac A, Herfray G. Expanding Boundaries - LCA Enhancement Perspectives to Facilitate Scaling up from Building to Territory – . [b] Sibiude G, Mailhac A, Herfray G, Schiopu N, Lebert A, Togo G, Villien P, Peuportier B, Valean C. vdf Hochschulverlag AG an der ETH Zürich. https://doi.org/10.3218/3774-6_42; 2016.

[33] Ross M. Fuel efficiency and the physics of automobiles. Contemp Phys 1997;38:381–94. https://doi.org/10.1080/001075197182199.

[34] Kim HC, Wallington TJ. Life cycle assessment of vehicle lightweighting: a physics-based model of mass-induced fuel consumption. Environ Sci Technol 2013;47:14358–66. https://doi.org/10.1021/es402954w.

[35] Geyer R, Malen DE. Parsimonious powertrain modeling for environmental vehicle assessments: part 1—internal combustion vehicles. Int J Life Cycle Assess 2020;25:1566–75. https://doi.org/10.1007/s11367-020-01774-0.

[36] Del Pero Francesco. Tool for the environmental assessment in the automotive context: analysis of the use stage for different typologies of LCA study. 2015.

[37] Koffler C, Rohde-Brandenburger K. On the calculation of fuel savings through lightweight design in automotive life cycle assessments. Int J Life Cycle Assess 2010;15:128–35. https://doi.org/10.1007/s11367-009-0127-z.

[38] Sovran. A contribution to understanding automotive fuel economy and its limits. 2003.

[39] Fontaras G, Zacharof N. Report on VECTO technology simulation capabilities and future outlook. 2016.

[40] Fiori C, Ahn K, Rakha HA. Power-based electric vehicle energy consumption model: model development and validation. Appl Energy 2016;168:257–68. https://doi.org/10.1016/j.apenergy.2016.01.097.

[41] Kneba Z, Stepanenko D, Rudnicki J. Numerical methodology for evaluation the combustion and emissions characteristics on WLTP in the light duty dual-fuel diesel vehicle. Combust Engines 2022;189:94–102. https://doi.org/10.19206/CE-143334.

[42] Miri I, Fotouhi A, Ewin N. Electric vehicle energy consumption modelling and estimation—A case study. Int J Energy Res 2021;45:501–20. https://doi.org/10.1002/er.5700.

[43] Ben-Chaim M, Shmerling E, Kuperman A. Analytic modeling of vehicle fuel consumption. Energies (Basel) 2013;6:117–27. https://doi.org/10.3390/en6010117.

[44] Khan Ankur A, Kraus S, Grube T, Castro R, Stolten D. A versatile model for estimating the fuel consumption of a wide range of transport modes. Energies (Basel) 2022;15:2232. https://doi.org/10.3390/en15062232.

[45] Sciarretta A, De Nunzio G, Ojeda LL. Optimal ecodriving control: energy-efficient driving of road vehicles as an optimal control problem. IEEE Control Syst 2015;35:71–90. https://doi.org/10.1109/MCS.2015.2449688.

[46] Del Pero F, Berzi L, Antonacci A, Delogu M. Automotive lightweight design: simulation modeling of mass-related consumption for electric vehicles. Machines 2020;8. https://doi.org/10.3390/machines8030051.

[47] Geyer R, Malen DE. Parsimonious powertrain modeling for environmental vehicle assessments: part 2—electric vehicles. Int J Life Cycle Assess 2020;25:1576–85. https://doi.org/10.1007/s11367-020-01775-z.

[48] Kim HC, Wallington TJ. Life cycle assessment of vehicle lightweighting: a physics-based model to estimate use-phase fuel consumption of electrified vehicles. Environ Sci Technol 2016;50:11226–33. https://doi.org/10.1021/acs.est.6b02059.

[49] Rohde-Brandenburger K, Koffler C, Reply to Kim, et al. Commentary on "Correction to: on the Calculation of fuel savings through lightweight design in

automotive life cycle assessments" by Koffler and Rohde-Brandenburger (2018). Int J Life Cycle Assess 2019;24:400–3. https://doi.org/10.1007/s11367-019-01585-y. 2019.
[50] Kim HC, Wallington TJ, Sullivan JL, Keoleian GA. Commentary on "Correction to: on the calculation of fuel savings through lightweight design in automotive life cycle assessments" by Koffler and Rohde-Brandeburger (2018). Int J Life Cycle Assess 2019;24:397–9. https://doi.org/10.1007/s11367-019-01584-z.
[51] Guzzella L, Onder CH. Introduction to modeling and control of internal combustion engine systems. Berlin, Heidelberg: Springer Berlin Heidelberg; 2010. https://doi.org/10.1007/978-3-642-10775-7.
[52] Pachernegg SJ. A closer look at the willans-line. https://doi.org/10.4271/690182; 1969.
[53] Rohde-Brandenburger K. Verbrauch in Fahrzyklen und im Realverkehr. Wiesbaden: Springer Fachmedien Wiesbaden; 2014. p. 243–306. https://doi.org/10.1007/978-3-658-04451-0_7. Energiemanagement im Kraftfahrzeug.
[54] Gebisa A, Gebresenbet G, Gopal R, Nallamothu RB. Driving cycles for estimating vehicle emission levels and energy consumption. Future Transport 2021;1:615–38. https://doi.org/10.3390/futuretransp1030033.
[55] Tutuianu M, Bonnel P, Ciuffo B, Haniu T, Ichikawa N, Marotta A, et al. Development of the World-Wide Harmonized Light duty Test Cycle (WLTC) and a possible pathway for its introduction in the European legislation. Transp Res D Transp Environ 2015;40:61–75. https://doi.org/10.1016/j.trd.2015.07.011.
[56] Weiss M, Bonnel P, Kühlwein J, Provenza A, Lambrecht U, Alessandrini S, et al. Will Euro 6 reduce the NOx emissions of new diesel cars? – insights from on-road tests with Portable Emissions Measurement Systems (PEMS). Atmos Environ 2012;62:657–65. https://doi.org/10.1016/j.atmosenv.2012.08.056.
[57] Sileghem L, Bosteels D, May J, Favre C, Verhelst S. Analysis of vehicle emission measurements on the new WLTC, the NEDC and the CADC. Transp Res D Transp Environ 2014;32:70–85. https://doi.org/10.1016/j.trd.2014.07.008.
[58] Nyberg P, Frisk E, Nielsen L. Driving cycle equivalence and transformation. IEEE Trans Veh Technol 2017;66:1963–74. https://doi.org/10.1109/TVT.2016.2582079.
[59] European Commission. Commission report under Article 12(3) of Regulation (EU) 2019/631 on the evolution of the real-world CO2 emissions gap for passenger cars and light commercial vehicles and containing the anonymised and aggregated real-world datasets referred to in Article 12 of Commission Implementing Regulation (EU) 2021/392. 2019.
[60] Fontaras G, Ciuffo B, Zacharof N, Tsiakmakis S, Marotta A, Pavlovic J, et al. The difference between reported and real-world CO 2 emissions: how much improvement can be expected by WLTP introduction? Transp Res Procedia 2017;25:3933–43. https://doi.org/10.1016/j.trpro.2017.05.333.
[61] Siano A, Vollero A, Conte F, Amabile S. "More than words": expanding the taxonomy of greenwashing after the Volkswagen scandal. J Bus Res 2017;71:27–37. https://doi.org/10.1016/j.jbusres.2016.11.002.
[62] Tran TB, Kolmanovsky I, Biberstein E, Makke O, Tharayil M, Gusikhin O. Wind sensitivity of electric vehicle energy consumption and influence on range prediction and optimal vehicle routes. 2023 IEEE international conference on mobility, operations, services and technologies (MOST). IEEE; 2023. p. 112–23. https://doi.org/10.1109/MOST57249.2023.00020.
[63] Swift A. Calculation of vehicle aerodynamic drag coefficients from velocity fitting of coastdown data. J Wind Eng Ind Aerod 1991;37:167–85. https://doi.org/10.1016/0167-6105(91)90071-4.
[64] Zemansky MW, Dittman RH. Heat and thermodynamics. sixth ed. New York: McGraw-Hill Books; 1981.
[65] Heywood J. Internal combustion engine fundamentals. second ed. McGraw Hill Education; 1988.
[66] Muranaka S, Tagaki Y, Ishida T. Factors limiting the improvement in thermal efficiency of S. I. Engine at higher compression ratio. SAE Trans 1987;96:526–36.
[67] Yagi S, Fujiwara K, Kuroki N, Maeda Y. Estimate of total engine loss and engine output in four stroke S.I. engines. SAE Trans 1991;100:530–41.
[68] Sandoval D, Heywood J. An improved friction model for spark-ignition engines. SAE Trans 2003;112:1041–52.
[69] EPA. Fuel economy guide. 2024.
[70] Mahmoudi A, Soong WL, Pellegrino G, Armando E. Efficiency maps of electrical machines. 2015 IEEE Energy Conversion Congress and Exposition (ECCE). IEEE; 2015. p. 2791–9. https://doi.org/10.1109/ECCE.2015.7310051.
[71] Roshandel E, Mahmoudi A, Kahourzade S, Yazdani A, Shafiullah G. Losses in efficiency maps of electric vehicles: an overview. Energies (Basel) 2021;14:7805. https://doi.org/10.3390/en14227805.
[72] Talbot D, Kahraman A, Li S, Singh A, Xu H. Development and validation of an automotive axle power loss model. Tribol Trans 2016;59:707–19. https://doi.org/10.1080/10402004.2015.1110862.
[73] Kunt MA. Analysis of the effect of different gearbox/transmission types on driveline friction losses by means of Gt suite simulation programme. Int J Automot Sci Technol 2021;5:271–80. https://doi.org/10.30939/ijastech..945675.
[74] Habermehl C, Jacobs G, Neumann S. A modeling method for gear transmission efficiency in transient operating conditions. Mech Mach Theor 2020;153:103996. https://doi.org/10.1016/j.mechmachtheory.2020.103996.
[75] Kostopoulos ED, Spyropoulos GC, Kaldellis JK. Real-world study for the optimal charging of electric vehicles. Energy Rep 2020;6:418–26. https://doi.org/10.1016/j.egyr.2019.12.008.
[76] Reick B, Konzept A, Kaufmann A, Stetter R, Engelmann D. Influence of charging losses on energy consumption and CO2 emissions of battery-electric vehicles. Vehicles 2021;3:736–48. https://doi.org/10.3390/vehicles3040043.
[77] Grunditz EA, Thiringer T. Performance analysis of current BEVs based on a comprehensive review of specifications. IEEE Transact Transport Electrificat 2016;2:270–89. https://doi.org/10.1109/TTE.2016.2571783.
[78] Ottaviano D. Technical assessment and modeling of lithium-ion batteries for electric vehicles. n.d.
[79] Lee D, Rousseau A, Rask E. Development and validation of the ford focus battery electric vehicle model. SAE Tech Papers 2014;1. https://doi.org/10.4271/2014-01-1809. SAE International.
[80] Ruan J, Walker PD, Watterson PA, Zhang N. The dynamic performance and economic benefit of a blended braking system in a multi-speed battery electric vehicle. Appl Energy 2016;183:1240–58. https://doi.org/10.1016/j.apenergy.2016.09.057.
[81] Mammosser D, Boisvert M, Micheau P. Designing a set of efficient regenerative braking strategies with a performance index tool. Proc Inst Mech Eng - Part D J Automob Eng 2014;228:1505–15. https://doi.org/10.1177/0954407014535918.
[82] Eberle R, Franze HA. Modelling the use phase of passenger cars in LCI. SAE Trans 1998:1998–2007.
[83] EPA - National Vehicle and Fuel Emissions Laboratory NC for ATechnology. ALPHA Map Package 2023.
[84] Dekraker P, Barba D, Moskalik A, Butters K. Constructing engine maps for full vehicle simulation modeling. https://doi.org/10.4271/2018-01-1412; 2018.
[85] Stuhldreher M. Fuel efficiency mapping of a 2014 6-Cylinder GM EcoTec 4.3L engine with cylinder deactivation. https://doi.org/10.4271/2016-01-0662; 2016.
[86] Moskalik A, Stuhldreher M, Kargul J. Benchmarking a 2018 Toyota camry UB80E eight-speed automatic transmission. https://doi.org/10.4271/2020-01-1286; 2020.
[87] Tsokolis D, Tsiakmakis S, Dimaratos A, Fontaras G, Pistikopoulos P, Ciuffo B, et al. Fuel consumption and CO2 emissions of passenger cars over the New Worldwide Harmonized Test Protocol. Appl Energy 2016;179:1152–65. https://doi.org/10.1016/j.apenergy.2016.07.091.
[88] https://ev-database.org/.EV-database. Consulted on 08-01-23 n.d.
[89] Vehicle Certification Agency. Car fuel data, CO2 and vehicle tax tools. https://CarfueldataVehicle-Certification-AgencyGovUk/, Consulted on 08-01-24 2020.
[90] European Environment Agency. EEA data: monitoring of CO2 emissions from passenger cars – regulation (EU) 2019/631. https://Co2carsAppsEeaEuropaEu/, Consulted on 08-01-24 2023.
[91] https://www.automobile-catalog.com.AutomobilCatalogDatabase. Consulted on 01/08/2024 n.d.
[92] International Council on Clean Transportation. The WLTP: how a new test procedure for cars will affect fuel consumption values in the EU. 2014.
[93] Yin Y, Wen H, Sun L, Hou W. The influence of road geometry on vehicle rollover and skidding. Int J Environ Res Publ Health 2020;17. https://doi.org/10.3390/ijerph17051648.
[94] Moawad A, Kim N, Shidore N, Rousseau A. Assessment of vehicle sizing, energy consumption, and cost through large-scale simulation of advanced vehicle technologies. 2016.
[95] Bishop JDK, Martin NPD, Boies AM. Cost-effectiveness of alternative powertrains for reduced energy use and CO2 emissions in passenger vehicles. Appl Energy 2014;124:44–61. https://doi.org/10.1016/j.apenergy.2014.02.019.
[96] Cox B, Bauer C, Mendoza Beltran A, van Vuuren DP, Mutel CL. Life cycle environmental and cost comparison of current and future passenger cars under different energy scenarios. Appl Energy 2020;269:115021. https://doi.org/10.1016/j.apenergy.2020.115021.
[97] SMMT. Smmt motor industry facts 2023. 2023.
[98] EPA. The 2022 EPA automotive trends report: greenhouse gas emissions. Fuel economy, and technology since 1975. 2022.
[99] Pineau P-O, Vincent B. Tendances du parc Automobile québécois 2013-2021. n.d.
[100] Díaz S, Rajon Bernard M, Bernard Y, Bieker G, Lee K, Mock P, et al. European vehicle market statistics 2020/2021. 2021.
[101] Nam EK, Sorab J. Friction reduction trends in modern engines. https://doi.org/10.4271/2004-01-1456; 2004.
[102] Levickis D, Gailis M, Rudzitis J, Kreicbergs J. Evaluation of methodology for determination of mechanical efficiency of spark ignition engine. https://doi.org/10.22616/ERDev2019.18.N300; 2019.
[103] Hjelkrem OA, Arnesen P, Aarseth Bø T, Sondell RS. Estimation of tank-to-wheel efficiency functions based on type approval data. Appl Energy 2020;276:115463. https://doi.org/10.1016/j.apenergy.2020.115463.
[104] Kamil M, Rahman MM, Bakar R A. An integrated model for predicting engine friction losses in internal combustion engines. Int J Automot Mech Eng 2014;9:1695–708. https://doi.org/10.15282/ijame.9.2013.19.0141.
[105] Hawkins TR, Singh B, Majeau-Bettez G, Strømman AH. Comparative environmental life cycle assessment of conventional and electric vehicles. J Ind Ecol 2013;17:53–64. https://doi.org/10.1111/j.1530-9290.2012.00532.x.
[106] Galvin R. Are electric vehicles getting too big and heavy? Modelling future vehicle journeying demand on a decarbonized US electricity grid. Energy Policy 2022;161:112746. https://doi.org/10.1016/j.enpol.2021.112746.
[107] Baran JK, Renneker CM, Malloy JD. All wheel drive efficiency testing. J. Passeng Cars 1988;97:805–14.
[108] Irimescu A, Mihon L, Pădure G. Automotive transmission efficiency measurement using a chassis dynamometer. Int J Automot Technol 2011;12:555–9. https://doi.org/10.1007/s12239-011-0065-1.
[109] Vantsevich VV. Power losses and energy efficiency of multi-wheel drive vehicles: a method for evaluation. J Terramechanics 2008;45:89–101. https://doi.org/10.1016/j.jterra.2008.08.001.

[110] Schwertner M, Weidmann U. Comparison of well-to-wheel efficiencies for different drivetrain configurations of transit buses. Transp Res Rec: J Transport Res Board 2016;2539:55–64. https://doi.org/10.3141/2539-07.
[111] Da Silva Gomes Pereira Correia MJ. Power loss modelling of a rear axle transmission with experimental study of No-load losses. 2017.
[112] Stańczyk TL, Prochowski L, Cegłowski D, Szumska EM, Ziubiński M. Assessment of driver performance and energy efficiency in transportation tasks when vehicle weight undergoes significant changes. Energies (Basel) 2023;16:5626. https://doi.org/10.3390/en16155626.
[113] Deligianni SP, Quddus M, Morris A, Anvuur A, Reed S. Analyzing and modeling drivers' deceleration behavior from normal driving. Transp Res Rec: J Transport Res Board 2017;2663:134–41. https://doi.org/10.3141/2663-17.
[114] Guillaume Saint Pierre, Lara Désiré. Driver's deceleration behaviour according to infrastructure. https://HalScience/Hal-040324692022.
[115] Karrouchi M, Nasri I, Rhiat M, Atmane I, Hirech K, Messaoudi A, et al. Driving behavior assessment: a practical study and technique for detecting a driver's condition and driving style. Transport Eng 2023;14:100217. https://doi.org/10.1016/j.treng.2023.100217.
[116] Riggins G, Bertini R, Ackaah W, Margreiter M. Evaluation of driver compliance to displayed variable advisory speed limit systems: Comparison between Germany and the U.S. Transp Res Procedia 2016;15:640–51. https://doi.org/10.1016/j.trpro.2016.06.054.
[117] SANEF. Résultats de l'Observatoire de SANEF des comportements sur autoroute. 2023.
[118] Observatoire National Interministériel de la Sécurité Routière Française. Observatoire des vitesses, Résultats de l'année 2018. 2018.
[119] Magnaval G, Boulay A-M. PETRAUL/Development of an analytical model of automobile energy consumption during use-phase for parametrized life cycle assessment (v.0.1). Zenodo 2025 [Data set].
[120] Lewis GM, Buchanan CA, Jhaveri KD, Sullivan JL, Kelly JC, Das S, et al. Green principles for vehicle lightweighting. Environ Sci Technol 2019;53:4063–77. https://doi.org/10.1021/acs.est.8b05897.
[121] Ghosh T, Kim HC, De Kleine R, Wallington TJ, Bakshi BR. Life cycle energy and greenhouse gas emissions implications of using carbon fiber reinforced polymers in automotive components: front subframe case study. Sustain Mater Technol 2021;28. https://doi.org/10.1016/j.susmat.2021.e00263.
[122] Shanmugam K, Gadhamshetty V, Yadav P, Athanassiadis D, Tysklind M, Upadhyayula VKK. Advanced high-strength steel and carbon fiber reinforced polymer composite body in white for passenger cars: environmental performance and sustainable return on investment under different propulsion modes. ACS Sustainable Chem Eng 2019;7:4951–63. https://doi.org/10.1021/acssuschemeng.8b05588.
[123] Cecchel S, Chindamo D, Collotta M, Cornacchia G, Panvini A, Tomasoni G, et al. Lightweighting in light commercial vehicles: cradle-to-grave life cycle assessment of a safety-relevant component. Int J Life Cycle Assess 2018;23:2043–54. https://doi.org/10.1007/s11367-017-1433-5.
[124] Delogu M, Del Pero F, Pierini M. Lightweight design solutions in the automotive field: environmental modelling based on fuel reduction value applied to diesel turbocharged vehicles. Sustainability 2016;8. https://doi.org/10.3390/su8111167.
[125] Kelly JC, Dai Q. Life-cycle analysis of vehicle lightweighting: a review. Electric, hybrid, and fuel cell vehicles. New York: Springer; 2021. p. 91–104. https://doi.org/10.1007/978-1-0716-1492-1_1080.
[126] Bulle C, Margni M, Patouillard L, Boulay AM, Bourgault G, De Bruille V, et al. Impact World+: a globally regionalized life cycle impact assessment method. Int J Life Cycle Assess 2019;24:1653–74. https://doi.org/10.1007/s11367-019-01583-0.